

## An Organic Receptor Isolated in an Unusual Intermediate Conformation: Computation, Crystallography and Hirshfeld Surface Analysis

Indravath Krishna Naik, Rudraditya Sarkar, Vedichi Madhu,  
Ramababu Bolligarla, Ravada Kishore, and Samar Kumar Das

*J. Phys. Chem. A*, **Just Accepted Manuscript** • DOI: 10.1021/acs.jpca.7b00091 • Publication Date (Web): 06 Apr 2017

Downloaded from <http://pubs.acs.org> on April 11, 2017

### Just Accepted

“Just Accepted” manuscripts have been peer-reviewed and accepted for publication. They are posted online prior to technical editing, formatting for publication and author proofing. The American Chemical Society provides “Just Accepted” as a free service to the research community to expedite the dissemination of scientific material as soon as possible after acceptance. “Just Accepted” manuscripts appear in full in PDF format accompanied by an HTML abstract. “Just Accepted” manuscripts have been fully peer reviewed, but should not be considered the official version of record. They are accessible to all readers and citable by the Digital Object Identifier (DOI®). “Just Accepted” is an optional service offered to authors. Therefore, the “Just Accepted” Web site may not include all articles that will be published in the journal. After a manuscript is technically edited and formatted, it will be removed from the “Just Accepted” Web site and published as an ASAP article. Note that technical editing may introduce minor changes to the manuscript text and/or graphics which could affect content, and all legal disclaimers and ethical guidelines that apply to the journal pertain. ACS cannot be held responsible for errors or consequences arising from the use of information contained in these “Just Accepted” manuscripts.



# An Organic Receptor Isolated in an Unusual Intermediate Conformation: Computation, Crystallography and Hirshfeld Surface Analysis

Indravath Krishna Naik, Rudraditya Sarkar, Vedichi Madhu, Ramababu Bolligarla, Ravada Kishore and Samar K. Das\*

*School of Chemistry, University of Hyderabad, Hyderabad 500 046, India*

**ABSTRACT:** 1,1''-1,4-phenylene-bis(methylene)bis-4,4'-bipyridinium cation  $[C_{28}H_{24}N_4]^{2+}$  (**c**), an organic receptor that generally crystallizes in its *anti*-conformation, has recently been shown to be isolated in its *syn*-conformation in an ion paired compound  $[C_{28}H_{24}N_4][Zn(dmit)_2] \cdot 2DMF$  ( $dmit^{2-} = 1,3$ -dithiole-2-thione-4,5-dithiolate). In this article, we have demonstrated that the same receptor  $[C_{28}H_{24}N_4]^{2+}$  (**c**) can also be stabilized in an unusual intermediate conformation (neither *syn* nor *anti*) with  $PF_6^-$  anion in compound  $[C_{28}H_{24}N_4](PF_6)_2 \cdot (1,4\text{-dioxane})$  (**1**·(**1,4-dioxane**)). The energetically favored *anti* conformation has been described in its nitrate salt  $[C_{28}H_{24}N_4](NO_3)_2 \cdot 2H_2O$  (**2**·**2H<sub>2</sub>O**). Compounds **1**·(**1,4-dioxane**) and **2**·**2H<sub>2</sub>O**, crystallizing in triclinic and monoclinic systems with space groups *P*-1 and *P*2<sub>1</sub>/*n* respectively, have additionally been characterized by Hirshfeld surface analysis. The density functional theory calculations are performed to understand the internal mechanism of the stability of various conformers of cationic receptor **c**, compound **1** and compound **2**. In conjunction with the electronic stability of the conformers, the natural bond orbital analysis and conformational equilibrium constants at different temperatures are also calculated to find out the sources of the different stability of the various conformers of experimentally synthesized compounds.

## ■ INTRODUCTION

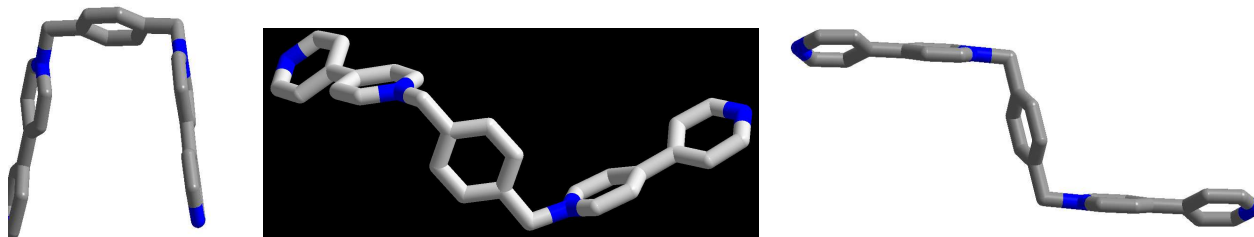
Intermolecular interactions in the solid state continue to be a topic of great interest in the field of supramolecular as well as materials chemistry because of its fundamental importance for the formation of higher organized chemical systems that result from the association of two or more chemical species.<sup>1-2</sup> Depending upon the function and need of selectivity in the molecular assembly processes, several types of weak but specific (mostly noncovalent) intermolecular interactions are involved that include ion pairing,<sup>3</sup> hydrogen bonding,<sup>4</sup> arene-arene ( $\pi$ - $\pi$ ) stacking interactions<sup>5-7</sup> etc. The biological processes,<sup>8-10</sup> that encounter such non-covalent interactions, are substrate-enzyme complex formation, the protein folding, the formation of membranes, antiportation of neutral and ionic species through membranes etc. In these intermolecular interactions, particularly between substrate and receptor (e.g., the active site of the enzyme), the receptor is generally flexible to undergo conformational changes to accommodate the substrate in an optimal geometry, comparable to 'lock-and-key fit' situation.<sup>11</sup>

Mimicking such conformational change using a specific substance is a great challenge to modern chemistry researchers. Many captivating, structurally diverse receptors (hosts) have been designed and synthesized for the purpose of studying the interactions between the receptor (host) and substrate (guest). Besides well-characterized macrocycles (hosts), e.g., cyclophanes,<sup>12</sup> cyclodextrins,<sup>13</sup> cryptophanes,<sup>14</sup> cucurbiturils,<sup>15</sup> carcerands,<sup>16</sup> supramolecular capsules<sup>17</sup> etc., acyclic compounds with cavities of flexible size, that are generally termed as molecular tweezers and clefts, proved to be effective synthetic receptors.<sup>18</sup> A molecular tweezer is defined as a synthetic receptor that contains two aromatic (complexing) chromophores connected by a single spacer. A cleft is nothing but a molecular tweezer having converged functional groups (receptors) that are separated by 10-12 Å (with the help of the spacer) to create a cavity for guest/substrate binding.<sup>19</sup> We report here an organic acyclic receptor cation having two aromatic side-arms (4,4'-bipyridines) connected by a single spacer (1,4-phenylene-bis(methylene)), namely, 1,1''-1,4-phenylene-bis(methylene)bis-4,4'-bipyridinium cation  $[C_{28}H_{24}N_4]^{2+}$  (**c**), which can interconvert between its *syn*- / (cleft-like) and *anti*- conformations as shown in Scheme 1 (left and right respectively). The receptor cation **c** can also be isolated in an unusual intermediate conformation (Scheme 1, middle). In this contribution, we have described synthesis and crystal structures of  $[C_{28}H_{24}N_4](PF_6)_2 \cdot (1,4\text{-dioxane})$  (**1**·(**1,4-dioxane**)) and  $[C_{28}H_{24}N_4](NO_3)_2 \cdot 2H_2O$  (**2**·**2H<sub>2</sub>O**) having an *intermediate* and *anti*-conformation respectively. The hexafluorophosphate

1  
2  
3 (PF<sub>6</sub><sup>-</sup>) salts of the same cation **c** have been reported earlier: in one of these, **c** is in *anti*-form<sup>20</sup>  
4 and in other salt,<sup>21</sup> **c** has a similar conformation, found in **1·(1,4-dioxane)**. However, both  
5 reports focused only on their respective crystal structures of the concerned hexafluorophosphate  
6 (PF<sub>6</sub><sup>-</sup>) salts including their supramolecular structures. We have undertaken this work to compare  
7 the *syn*- and *anti*-conformations of **c** in **1·(1,4-dioxane)** and **2·2H<sub>2</sub>O** respectively emphasizing  
8 the role of hydrogen bonding of surrounding anions. We have also performed Hirshfeld surface  
9 analyses on the crystal structures of **1·(1,4-dioxane)** and **2·2H<sub>2</sub>O** to rationalize the molecular  
10 conformations of **c** in their respective salts.  
11

12  
13  
14  
15  
16  
17  
18 In order to understand the unusual conformation of the cation **c** in compound **1·(1,4-**  
19 **dioxane)**, we performed quantum mechanical calculations using density functional theory and  
20 we tried to understand internal mechanism of the stability of different conformers of the cationic  
21 receptor **c**, compound **1** and compound **2**. The electronic stability of the conformers were  
22 analyzed by considering isodesmic reaction between the cationic receptor **c** and donor anions,  
23 PF<sub>6</sub><sup>-</sup> and NO<sub>3</sub><sup>-</sup>, following the principles of thermodynamics. The different conformational  
24 analyses of the compound **1** have been performed by fixing the 1N-24C-52C-29N dihedral angle  
25 at different values (see in the text for details). On the other hand, stability of these compounds on  
26 excitation is also measured by evaluating the energy gap between highest occupied molecular  
27 orbital (HOMO) and lowest unoccupied molecular orbital (LUMO) at the electronic ground state  
28 of the respective compounds. The possible interactions between the occupied donor orbitals and  
29 unoccupied acceptor orbitals in these compounds are also calculated by using second-order  
30 perturbation theory as implemented in natural bond orbital analysis (NBO). As a result of these  
31 analyses, the sources of the different stabilities of the various conformers of the respective  
32 compounds can be accounted and results are discussed in details in the text. At last, we  
33 calculated the equilibrium constants of various conformational equilibria among the different  
34 conformers of the respective compounds to confirm the results of the above analyses by taking  
35 the experimental conformational equilibrium constant values between the *cis*-2-butene and *trans*-  
36 2-butene at different temperature as a reference.  
37  
38  
39  
40  
41  
42  
43  
44  
45  
46  
47  
48  
49  
50  
51  
52  
53  
54  
55  
56  
57  
58  
59  
60

Scheme 1

*Syn- / Cleft-like**Intermediate**Anti-*

## ■ EXPERIMENTAL, PHYSICAL AND THEORETICAL METHODS

**Physical measurements.** All reagents and solvents were commercially available and used without further purification. Elemental analysis (C, H and N) were obtained with a FLASH EA 1112 Series CHNS analyser. FT-IR spectra were recorded in the range 400-4000  $\text{cm}^{-1}$  with a JASCO FT/IR-5300 spectrometer using KBr pellet.  $^1\text{H}$  NMR spectra were recorded on Bruker DRX- 400 spectrometer using  $\text{Si}(\text{CH}_3)_4$  as an internal standard.

**Synthesis of compound  $[\text{C}_{28}\text{H}_{24}\text{N}_4](\text{PF}_6)_2 \cdot (1,4\text{-dioxane})$  (**1**·(1,4-dioxane)).** 150 mg (0.568 mmol) of 1,4-bis(bromomethyl)benzene, dissolved in 10 mL of dry acetonitrile, were added dropwise to a refluxing solution of 4,4'-bipyridine (500 mg, 3.2 mmol) in 10 mL of acetonitrile. The reaction mixture was then refluxed for additional 2 h. The  $[\text{C}_{28}\text{H}_{24}\text{N}_4]\text{Br}_2$  salt came out as insoluble white solid. The precipitate was washed with acetonitrile and dried in vacuum. This product was then dissolved in warm water and subsequently, it was treated with  $\text{NH}_4\text{PF}_6$ . This results in the precipitation of  $[\text{C}_{28}\text{H}_{24}\text{N}_4](\text{PF}_6)_2$  (1,1'-1,4-phenylene-bis(methylene)bis-4,4'-bipyridinium-bis(hexafluorophosphate). Yield: 0.276 g (~70%). This can be described as crude  $\text{PF}_6$  salt of **c**,  $[\text{C}_{28}\text{H}_{24}\text{N}_4](\text{PF}_6)_2$ . This crude product was recrystallized by the vapor diffusion of diethylether into a solution of  $[\text{C}_{28}\text{H}_{24}\text{N}_4](\text{PF}_6)_2$  in a mixed solvents of DMF:1,4-dioxane (1:3) into the single crystals of  $[\text{C}_{28}\text{H}_{24}\text{N}_4](\text{PF}_6)_2 \cdot (1,4\text{-dioxane})$  (**1**·(1,4-dioxane)). Anal. Calcd. for  $(\text{C}_{32}\text{H}_{32}\text{F}_{12}\text{N}_4\text{O}_2\text{P}_2)$ : C, 48.37; H, 4.06; N, 7.05. Found: C, 48.26; H, 4.11; N, 7.12. IR (KBr pellet) ( $\nu/\text{cm}^{-1}$ ): 3134s, 3074w, 2150w, 1699m, 1639s, 1502m, 1460s, 1421m, 1215s, 1184m, 1010m, 835s, 557s, 515w.  $^1\text{H}$  NMR ( $\text{DMSO}-d_6$ ):  $\delta$  9.28(d,  $J=6.647$ , 4H); 8.81(d,  $J=6.51$ , 4H);

8.62(d, J=6.48, 4H); 7.97(d, J=6.491, 4H); 7.66(S, 4H); 5.89(S, 4H).

**Synthesis of compound [C<sub>28</sub>H<sub>24</sub>N<sub>4</sub>](NO<sub>3</sub>)<sub>2</sub>·2H<sub>2</sub>O (2·2H<sub>2</sub>O).** Compound **2·2H<sub>2</sub>O** was synthesized by an ion exchange method as follows: 0.07 g (0.1 mmol) of [C<sub>28</sub>H<sub>24</sub>N<sub>4</sub>](PF<sub>6</sub>)<sub>2</sub> was taken in a 10mL round bottom flask and 0.034 g (0.2 mmol) of AgNO<sub>3</sub> was taken in an another 10mL round bottom flask. Then the two round bottom flasks were fitted into two terminals of a λ-shaped glass tube. Then the whole λ tube was filled by CH<sub>3</sub>CN solution keeping the whole system closed. After two weeks, colorless needle-shaped crystals of [C<sub>28</sub>H<sub>24</sub>N<sub>4</sub>](NO<sub>3</sub>)<sub>2</sub> · 2H<sub>2</sub>O (**2·2H<sub>2</sub>O**) were deposited on the top of the λ tube. Yield: 0.048 g (84%). Anal. Calcd. for (C<sub>28</sub>H<sub>28</sub>N<sub>6</sub>O<sub>8</sub>): C, 58.33; H, 4.89; N, 14.58. Found: C, 58.26; H, 4.95; N, 14.49. IR (KBr pellet) ( $\nu/\text{cm}^{-1}$ ) for **2·2H<sub>2</sub>O**: 3323m, 3107w, 3020w, 1633s, 1593w, 1545m, 1523m, 1493m, 1350 (NO<sub>3</sub><sup>-</sup>)s, 1211w, 1161m, 1070w, 895w, 823s, 771s, 727m, 513m, 478w.

**X-ray crystallography.** [C<sub>28</sub>H<sub>24</sub>N<sub>4</sub>](PF<sub>6</sub>)<sub>2</sub>·(1,4-dioxane) (**1·(1,4-dioxane)**) was measured at 100 K and [C<sub>28</sub>H<sub>24</sub>N<sub>4</sub>](NO<sub>3</sub>)<sub>2</sub> · 2H<sub>2</sub>O (**2·2H<sub>2</sub>O**) was measured at 298 K on a Bruker SMART APEX CCD area detector system [ $\lambda(\text{Mo-K}\alpha) = 0.71073 \text{ \AA}$ ] with a graphite monochromator. 2400 frames were recorded with an  $\omega$  scan width of 0.3°, each for 8 s. Crystal-detector distance was 60 mm with a collimator of 0.5 mm. The SMART software<sup>22</sup> was used for intensity data acquisition and the SAINTPLUS software<sup>22</sup> was used for data extraction. Absorption correction was performed with the help of SADABS program.<sup>22</sup> Programs of SHELX-97<sup>23</sup> were used for structure solution by direct methods and least-square refinement on F<sup>2</sup>. All non-hydrogen atoms were refined anisotropically. Hydrogen atoms on aromatic ring were introduced on calculated positions and included in the refinement riding on their respective parent atoms. We tried to locate the hydrogen atoms of solvent water molecules in the crystal structure of compound **2·2H<sub>2</sub>O** through differential Fourier maps, but could not succeed. Therefore the O–H···O hydrogen bonding distances in the supramolecular structure of water in compound **2·2H<sub>2</sub>O** have been described as O···O separations (taking O···O distance in the range of 2.395 Å to 2.950 Å). Detailed information about crystal data and structure determination are summarized in Table 1.

**Computational methods.** Computational simulations of the different conformers of cationic receptor **c**, compound **1** and compound **2** were performed with density functional theory (DFT) as implemented in Gaussian 09<sup>24</sup> suite programming package. Computational data

1  
2  
3 evaluation through out the present study were performed with B3LYP hybrid functional,<sup>25-29</sup>  
4 which includes Hartree-Fock (HF) exchange as well as DFT exchange correlations. The non-  
5 local correlations part is taken care by Lee, Yang and Parr (LYP) functional. All calculations  
6 were performed using Pople's 6-31G(d,p) basis set. The calculations of minimum energy  
7 conformers of the cationic receptor **c**, compound **1** and compound **2** were confirmed by  
8 subsequent frequency calculations of the optimized geometry at the ground state of the  
9 respective conformers. We note that no imaginary frequency was found at the optimized  
10 geometry of the conformers. The first thirty-four lowest frequencies of each conformer are given  
11 in **Table S1** in the supporting information.

12  
13  
14  
15  
16  
17  
18  
19  
20  
21  
22  
23  
24  
25  
26  
27  
28  
29  
30  
31  
32  
33  
34  
35  
36  
37  
38  
39  
40  
41  
42  
43  
44  
45  
46  
47  
48  
49  
50  
51  
52  
53  
54  
55  
56  
57  
58  
59  
60

Natural bond orbital (NBO) analysis was performed to find out the different intra molecular interactions in cationic receptor **c**, compound **1** and compound **2**. The possible interaction between the filled donor orbital (i) and vacant acceptor orbital (j) was accounted in the NBO analysis. The stabilization energy of the donor-acceptor interaction  $[E^{(2)}(i,j)]$  was calculated by second-order perturbation theory. The stabilization energy  $[E^{(2)}(i,j)]$  associated with the electron delocalization between the donor (i) and acceptor (j) orbitals can be expressed as:

$$E^{(2)}(i,j) = q_i \frac{[F(i,j)]^2}{E_j - E_i} \quad (1)$$

Where,  $q_i$  is the orbital occupancy,  $E_i$ ,  $E_j$  are diagonal elements and  $F_{ij}$  are the off-diagonal elements of the NBO Fock matrix.

Equilibrium constant (K) between the different conformers of cationic receptor **c** and compound **1** were calculated by considering the ratio of number of reactant (r, more stable conformer) and product (p, less stable conformer) molecules at equilibrium.<sup>25-29</sup> The ratio of r and p can be expressed as:

$$\frac{N_p}{N_r} = \left( \frac{q_p}{q_r} \right) e^{-\frac{\Delta E}{RT}} \quad (2)$$

Where,  $N_p$ ,  $N_r$  are the number of product and reactant molecules at equilibrium. The partition functions of the product and reactant are designated as  $q_p$ ,  $q_r$ , respectively.  $\Delta E$  is the total energy difference between the reactant and product and R is the universal gas constant. T represents the temperature in Kelvin. So the equilibrium constant of these conformers can be expressed as:

$$K = \left( \frac{q_p}{q_r} \right) e^{-\frac{\Delta E}{RT}} \quad (3)$$

or,

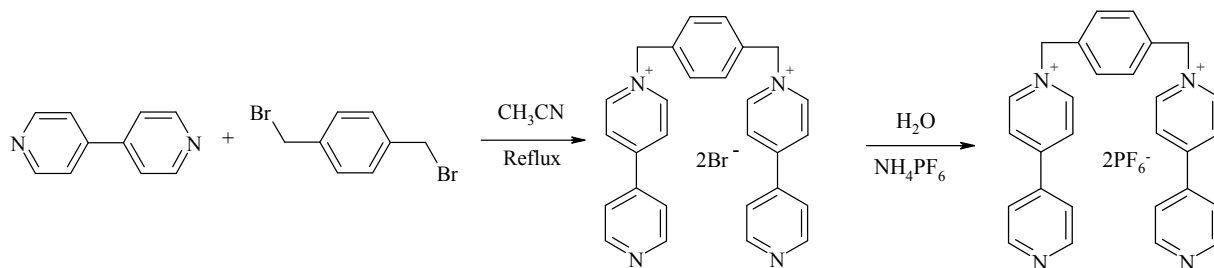
$$K = \left( \frac{q_p^{\text{vib}} q_p^{\text{rot}}}{q_r^{\text{vib}} q_r^{\text{rot}}} \right) e^{-\frac{\Delta E}{RT}} \quad (4)$$

Where  $q_p^{\text{vib}}$ ,  $q_p^{\text{rot}}$ ,  $q_r^{\text{vib}}$  and  $q_r^{\text{rot}}$  are the vibrational and rotational partition functions of the product and reactant, respectively. The translational partition functions of reactant and product are equal and hence cancel out. The electronic ground states of product and reactant are non-degenerate; hence electronic partition function is unity. To validate the above Eq. (4), we calculated the equilibrium constants (K) between cis-2-butene and trans-2-butene, conformers of 2-butene at different temperatures and compared with the available experimental values.<sup>30</sup> The calculated rotational constants, symmetry numbers of these conformers are given in **Table S2** in the Supporting information. The rotational and vibrational partition functions of these conformers at different temperature are given in **Table S3** in the Supporting information. This comparison between the experimental and theoretical K values of cis-2-butene  $\rightleftharpoons$  trans-2-butene equilibrium at different temperatures is given in **Table S4** in the Supporting information. It is found that theoretically evaluated K values between cis-2-butene and trans-2-butene equilibrium are in good accord with the experimental values.<sup>30</sup> The values of rotational constants, symmetry number,  $q^{\text{rot}}$  and  $q^{\text{vib}}$  of the conformers of cationic receptor, compound **1** and compound **2** are also given in the **Tables S2** and **S3** in the Supporting information to make the theoretical analysis more easier in latter sections.

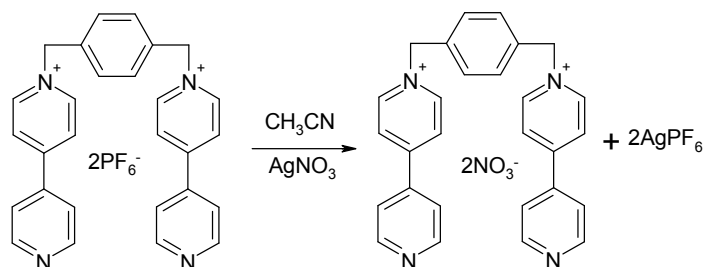
## ■ RESULTS AND DISCUSSION

**Synthesis.** The crude  $[C_{28}H_{24}N_4](PF_6)_2$  is synthesized from 1,4-bis(bromomethyl)benzene and 4,4'-bipyridine (Scheme 2). This crude solid is then crystallized from DMF-1,4-dioxane to obtain the single crystals of compound  $[C_{28}H_{24}N_4](PF_6)_2 \cdot (1,4\text{-dioxane})$  (**1**·(**1,4-dioxane**)). The nitrate salt (compound **2**·**2H<sub>2</sub>O**) could not be synthesized from a direct method, but this can be

## Scheme 2

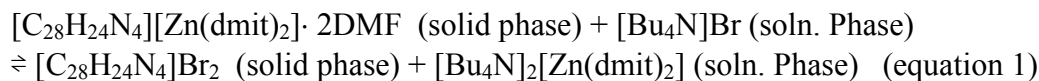


## Scheme 3



prepared from the crude  $\text{PF}_6^-$ -salt of compound 1.(1,4-dioxane) by an ion exchange method with silver nitrate (Scheme 3). Compounds **1** and **2** have been characterized by IR spectral studies,  $^1\text{H}$  NMR studies including elemental analyses and finally unambiguously by single crystal X-ray crystallography.

**Crystal structure description and discussion.** The bromide salt of the title cationic receptor  $[\text{C}_{28}\text{H}_{24}\text{N}_4]^{2+}$  (**c**),  $[\text{C}_{28}\text{H}_{24}\text{N}_4]\text{Br}_2$  was structurally characterized and the usual *anti*-conformation of the cation **c** (Scheme 1, right) is found in the crystal structure of  $[\text{C}_{28}\text{H}_{24}\text{N}_4]\text{Br}_2$ .<sup>21</sup> When these off-white crystals of  $[\text{C}_{28}\text{H}_{24}\text{N}_4]\text{Br}_2$  are suspended in MeCN solvent with few drops of DMF (**c**) crystals are not soluble in this medium) dissolving an excess amount of  $[\text{Bu}_4\text{N}]_2[\text{Zn}(\text{dmit})_2]$  and stirred for about a week, the off-white solid of  $[\text{C}_{28}\text{H}_{24}\text{N}_4]\text{Br}_2$  becomes dark brown with the conversion of  $[\text{C}_{28}\text{H}_{24}\text{N}_4][\text{Zn}(\text{dmit})_2]$  in a solid-liquid interface crystalline state reaction. In the red-brown solid of compound  $[\text{C}_{28}\text{H}_{24}\text{N}_4][\text{Zn}(\text{dmit})_2]$ , the cationic receptor  $[\text{C}_{28}\text{H}_{24}\text{N}_4]^{2+}$  (**c**) has *syn*-conformation (Scheme 1, left), as observed in the crystal structure of  $[\text{C}_{28}\text{H}_{24}\text{N}_4][\text{Zn}(\text{dmit})_2] \cdot 2\text{DMF}$ .<sup>31</sup> By exploiting the flexible nature of this acyclic cationic receptor  $[\text{C}_{28}\text{H}_{24}\text{N}_4]^{2+}$  (**c**), we could demonstrate the reversible *syn-anti* conformational change of **c** in solid to solid antiformations (equation 1). We wanted to exploit further the flexible nature of  $[\text{C}_{28}\text{H}_{24}\text{N}_4]^{2+}$



(c) by crystallizing this cation with diverse anions and we synthesized compound  $[C_{28}H_{24}N_4](PF_6)_2 \cdot (1,4\text{-dioxane})$  (**1·(1,4-dioxane)**) (with  $PF_6^-$  anion) and compound  $[C_{28}H_{24}N_4](NO_3)_2 \cdot 2H_2O$  (**2·2H<sub>2</sub>O**) (with  $NO_3^-$  anion).

Compound  $C_{28}H_{24}N_4](PF_6)_2 \cdot (1,4\text{-dioxane})$  (**1·(1,4-dioxane)**) crystallizes in the triclinic system with space group *P-1* and concerned single crystal X-ray data parameters, obtained at 100 K, are described in Table 1. The thermal ellipsoidal plot of the compound **1·(1,4-dioxane)** is displayed in Figure 1 and the relevant selected bond lengths and angles are described in Table 2. Interestingly, the cation **c**, observed in the crystal structure of  $C_{28}H_{24}N_4](PF_6)_2 \cdot (1,4\text{-dioxane})$  (**1·(1,4-dioxane)**) adopts an intermediate conformation which is in-between *syn*- and *anti*-

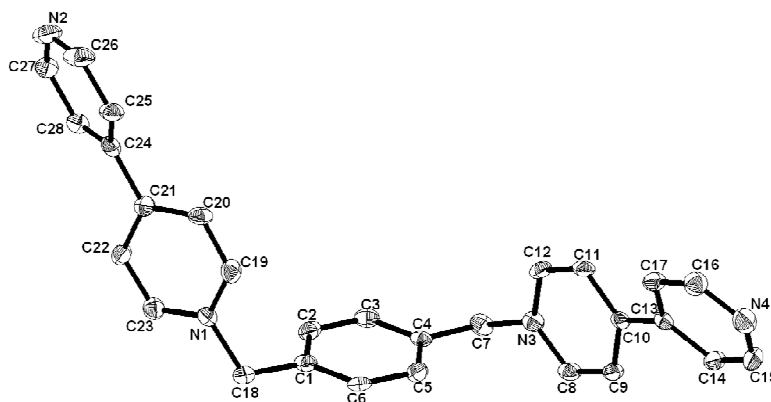


**Figure 1** Thermal ellipsoidal plot (30 % probability) of organic receptor  $[C_{28}H_{24}N_4]^{2+}$  in compound  $[C_{28}H_{24}N_4](PF_6)_2 \cdot (1,4\text{-dioxane})$  (**1·(1,4-dioxane)**); anions, solvent molecules and hydrogens are omitted for clarity.

conformations (Scheme 1, middle and Figure 1). We believe that inter-cation-anion hydrogen bonding interactions (mostly  $C-H \cdots F$  hydrogen bonds) between the cation receptor **c** and anion  $PF_6^-$  are responsible for this unusual intermediate conformation of **c** in the crystal structure of compound **1·(1,4-dioxane)**. The  $C-H \cdots F$  hydrogen bonding environment around the  $PF_6^-$  anion is given in Figure 2. The relevant hydrogen bonding parameters are presented in Table 3. In other words, in the crystal structure, the stability of intermediate conformation (between *syn* and *anti*)

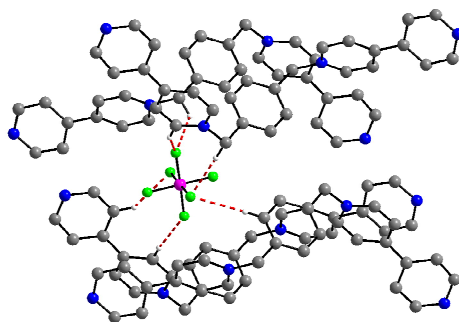


**Figure 2.** C-H...F hydrogen bonding environment around a PF<sub>6</sub> anion in [C<sub>28</sub>H<sub>24</sub>N<sub>4</sub>](PF<sub>6</sub>)<sub>2</sub>·(1,4-dioxane) (**1**·(**1,4-dioxane**)).

of the organic receptor [C<sub>28</sub>H<sub>24</sub>N<sub>4</sub>]<sup>2+</sup> (**c**) in compound [C<sub>28</sub>H<sub>24</sub>N<sub>4</sub>](PF<sub>6</sub>)<sub>2</sub>·(1,4-dioxane) (**1**·(**1,4-dioxane**)) can be rationalized by its strong hydrogen bonding interactions with surrounding PF<sub>6</sub><sup>-</sup> anions resulting in a three-dimensional supramolecular network that have well-defined void spaces, occupied by the solvent 1,4-dioxane molecules as shown in Figure 3. We have also performed density functional theory (DFT) calculations to understand this intermediate conformation of **c** in compound **1**·(**1,4-dioxane**) (*vide infra*).

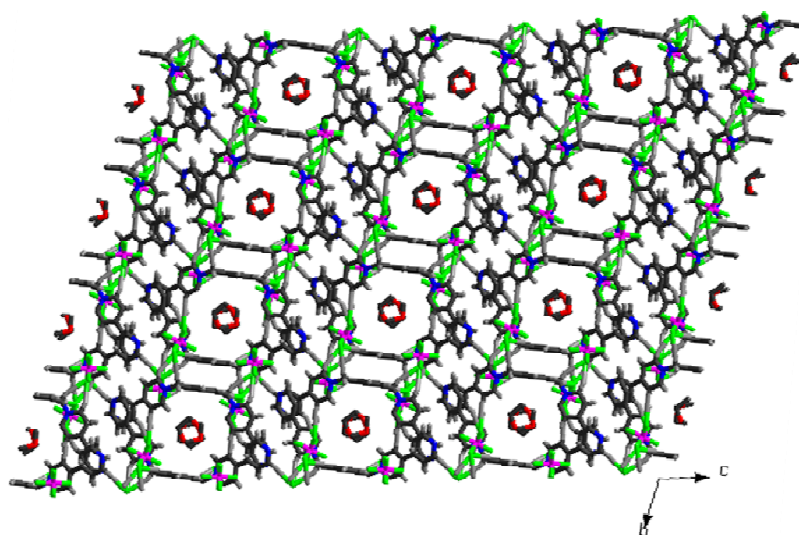


**Figure 3.** View (wire-frame representation) of the molecular packing of [C<sub>28</sub>H<sub>24</sub>N<sub>4</sub>](PF<sub>6</sub>)<sub>2</sub>·(1,4-dioxane) (**1**·(**1,4-dioxane**)) (4×4) cells; color code: F, green; P, purple; C, gray; N, blue; O, red; H, medium gray.

Compound [C<sub>28</sub>H<sub>24</sub>N<sub>4</sub>](NO<sub>3</sub>)<sub>2</sub> · 2H<sub>2</sub>O (**2**·**2H<sub>2</sub>O**) crystallizes in monoclinic system with space group *P2<sub>1</sub>/n*. The X-ray analysis of a single crystal of compound **2**·**2H<sub>2</sub>O** reveals that the dication [C<sub>28</sub>H<sub>24</sub>N<sub>4</sub>]<sup>2+</sup> (**c**) adopts an usual *anti*-conformation with respect to the two bipyridine units of the para-xylene ring as shown in Figure 4. In the asymmetric unit of the concerned

crystal structure, one lattice water molecule (O4, located in a general position) exists with half of the cationic receptor (c) and one nitrate anion. Thus the molecular formula of compound  $2 \cdot 2\text{H}_2\text{O}$  consists of a full molecule of cationic receptor, two nitrate anions and two lattice water molecules.

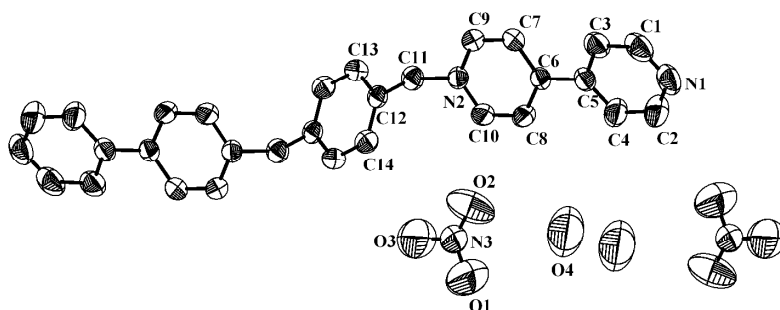


**Figure 4.** Thermal ellipsoidal plot of the asymmetric unit of compound  $[\text{C}_{28}\text{H}_{24}\text{N}_4](\text{NO}_3)_2 \cdot 2\text{H}_2\text{O}$  ( $2 \cdot 2\text{H}_2\text{O}$ ), hydrogen atoms are not shown for clarity (50% probability).

Interestingly, the solvent water molecule (O4) arranges in the form of a water chain (a centro-symmetric array) with two different hydrogen bonding distances (2.395 Å and 2.678 Å). A small fragment of the chain is formed by the hydrogen bonding interaction (2.395 Å) between O4 and O4(a) (Figure 5a, left). These fragments are connected further by a relatively larger H-bond distance (2.678 Å) to form the water chain (Figure 5a, right).

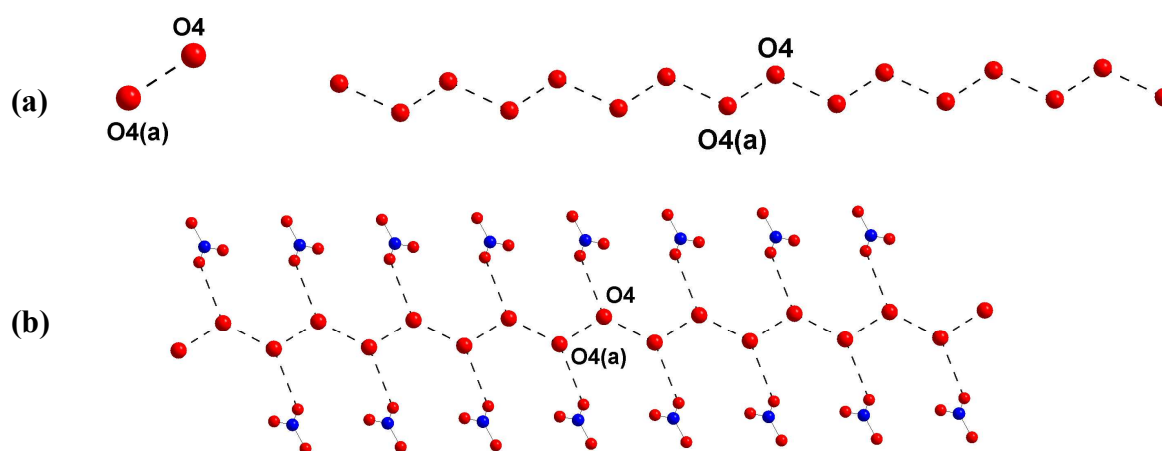


**Figure 5.** (a) left: Supramolecular water dimer and right: its one-dimensional chain-like arrangement formed from hydrogen bonding interactions of O4 and O4(a), that are related by a symmetry operation: a, 2-x, 1-y, -z. (b) Extended water structure formed from the solvent water molecule (O4), showing its hydrogen bonding interactions with its surrounding nitrate anions.

Each water molecule of this water chain is further hydrogen bonded (2.912 Å) to an oxygen atom (O2) of the surrounding nitrate anion (Figure 5(b)). In the crystal structure of compound  $[\text{C}_{28}\text{H}_{24}\text{N}_4](\text{NO}_3)_2 \cdot 2\text{H}_2\text{O}$  (**2·2H<sub>2</sub>O**), the stair-case-like (*anti*-conformation) dications  $[\text{C}_{28}\text{H}_{24}\text{N}_4]^{2+}$  (c) pack to form zig-zag arrays with two nitrate anions and two crystal water molecules, inserted in between the dications as shown in Figure 6(a). The corresponding space filling plot (without nitrate anions and lattice water molecules) is shown in Figure 6(b).

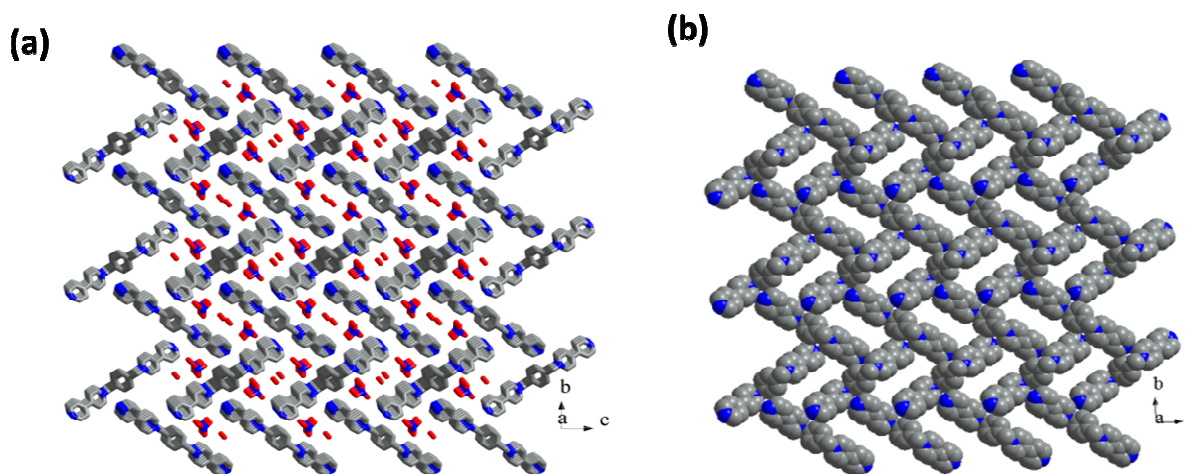


**Figure 6.** (a) Packing diagram consisting of the dication  $[\text{C}_{28}\text{H}_{24}\text{N}_4]^{2+}$ ,  $\text{NO}_3^-$  anion and crystal water molecules in **2·2H<sub>2</sub>O**. Hydrogen atoms are not shown for clarity. (b) View (face filling representation) of the molecular packing of  $[\text{C}_{28}\text{H}_{24}\text{N}_4]^{2+}$  cations in the  $[\text{C}_{28}\text{H}_{24}\text{N}_4][\text{NO}_3]_2 \cdot 2\text{H}_2\text{O}$  (**2·2H<sub>2</sub>O**) (3×3) cells. Color code: N, blue; C, gray; O, red. The hydrogen atoms, nitrate anions and water molecules are not shown for clarity

**Organic receptor  $[\text{C}_{28}\text{H}_{24}\text{N}_4]^{2+}$  (c) take up its usual *anti*-conformation in compound **2·2H<sub>2</sub>O** (nitrate salt) and is stabilized in an unusual *intermediate*-conformation in compound **1·(1,4-dioxane)** ( $\text{PF}_6^-$  salt)! Why is it so? A supramolecular analysis from respective crystal structures.**

The usual energetically favored conformation of the cationic receptor  $[\text{C}_{28}\text{H}_{24}\text{N}_4]^{2+}$  (c) is *anti*, observed in the crystal structure of compound  $[\text{C}_{28}\text{H}_{24}\text{N}_4](\text{NO}_3)_2 \cdot 2\text{H}_2\text{O}$  (**2·2H<sub>2</sub>O**). The deviation from this usual *anti*-conformation of c can be explained by considering supramolecular hydrogen bonding interactions of this dication (c) with its surrounding anions ( $\text{PF}_6^-$  anion in case of compound **1·(1,4-dioxane)** and  $\text{NO}_3^-$  anion in the case of compound **2·2H<sub>2</sub>O**). The supramolecular hydrogen bonding interactions around the cationic receptor (c) can be ‘balanced’ as well as ‘unbalanced’. The receptor c is flexible and it can undergo conformational change from *anti* (Scheme 1, right) to an *intermediate* (Scheme 1, middle) through *syn* (Scheme 1, left).

1  
2  
3  
4  
5  
6  
7  
8  
9  
10  
11  
12  
13  
14  
15  
16  
17  
18  
19  
20  
21  
22  
23  
24  
25  
26  
27  
28  
29  
30  
31  
32  
33  
34  
35  
36  
37  
38  
39  
40  
41  
42  
43  
44  
45  
46  
47  
48  
49  
50  
51  
52  
53  
54  
55  
56  
57  
58  
59  
60

However, this movement (conformational change) can be restricted by the number of supramolecular interactions with its surrounding anions. As shown in Figure 7(a), there are unbalanced supramolecular H-bonding interactions around the di-cation **c**; the unbalanced supramolecular interactions mean un-equivalent interactions with respect to the central part of the molecule. This di-cation has two bipyridine side arms with respect to the central phenylene ring. In the case of compound **1**·(1,4-dioxane), one side arm is involved with five C–H···F hydrogen bonds and the other side arm is involved in six C–H···F hydrogen bonds as shown in Figure 7(a). These un-equivalent supramolecular hydrogen bonding interactions, called unbalanced supramolecular interactions, around **c** enable this system to adopt an unusual intermediate conformation (Scheme 1, middle). The supramolecular hydrogen bonding interactions around **c** in compound [C<sub>28</sub>H<sub>24</sub>N<sub>4</sub>](NO<sub>3</sub>)<sub>2</sub> · 2H<sub>2</sub>O (**2**·2H<sub>2</sub>O) is shown in Figure 7(b). In the crystal structure of compound **2**·2H<sub>2</sub>O, there are balanced/equivalent C–H···O hydrogen bonding interactions around **c** with respect to the central phenylene ring (Figure 7(b)). Both side arms of **c** are hydrogen bonded with its surrounding NO<sub>3</sub><sup>−</sup> anions in such a way that hydrogen bonding force of one arm would cancel that of other arm. Thus there is an equivalent force along all the sides of cationic receptor [C<sub>28</sub>H<sub>24</sub>N<sub>4</sub>]<sup>2+</sup> (**c**), which implies that there is no more distortion from its usual *anti*-conformation. This justifies the *anti*-conformation of **c** in compound **2**·2H<sub>2</sub>O. The *anti*-conformation of **c** in compound **2**·2H<sub>2</sub>O and an *intermediate* conformation of **c** in compound **1** can also be corroborated by DFT calculations, Hirshfeld surface analysis and 2D finger plots, described in the succeeding sections.

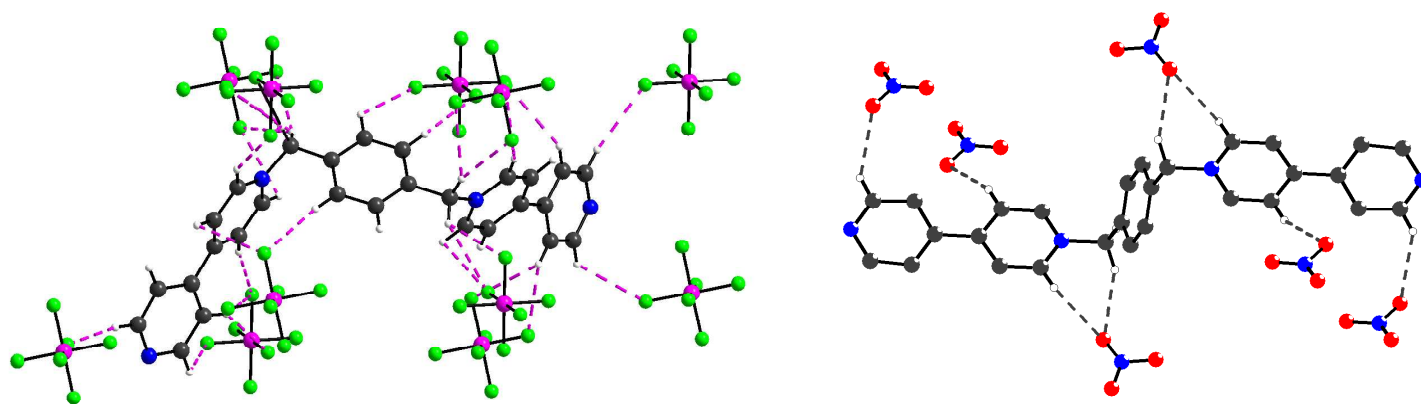


**Figure 7.** (a) Unbalanced/unsymmetrical C–H···F hydrogen bonding interactions around the cationic receptor [C<sub>28</sub>H<sub>24</sub>N<sub>4</sub>]<sup>2+</sup>, observed in the crystal structure of compound [C<sub>28</sub>H<sub>24</sub>N<sub>4</sub>](PF<sub>6</sub>)<sub>2</sub>·(1,4-dioxane) (**1**·(1,4-dioxane)). (b) Balanced/symmetrical C–H···O hydrogen bonding interactions around C<sub>28</sub>H<sub>24</sub>N<sub>4</sub>]<sup>2+</sup>, found in the crystal of compound [C<sub>28</sub>H<sub>24</sub>N<sub>4</sub>](NO<sub>3</sub>)<sub>2</sub>·2H<sub>2</sub>O (**2**·2H<sub>2</sub>O)

**Hirshfeld Surface Analysis.** The hydrogen-bonding supramolecular interactions around the cationic receptor  $[C_{28}H_{24}N_4]^{2+}$  (c) with surrounding associated anions are further analyzed with the Hirshfeld Surfaces (HSs) and 2D fingerprint plots (FPs), which are generated by using the software Crystal explorer 3.1.<sup>32,33</sup> based on the pertinent CIF files. Hirshfeld surfaces mapped with different properties e.g.,  $d_e$ ,  $d_{norm}$ , shape index, curvedness, have been proven to be an useful visualization tool for the analysis of supramolecular intermolecular interactions and crystal packing behavior of molecules.<sup>34,35</sup> The 3D Hirshfeld surfaces offer more insight into long- and short-range interactions, experienced by the relevant molecules, and 2D finger plots, derived from the HSs provide the nature, type and relative contribution of the intermolecular interactions. The HSs of the present cationic receptor  $[C_{28}H_{24}N_4]^{2+}$  (c) experiences unbalanced

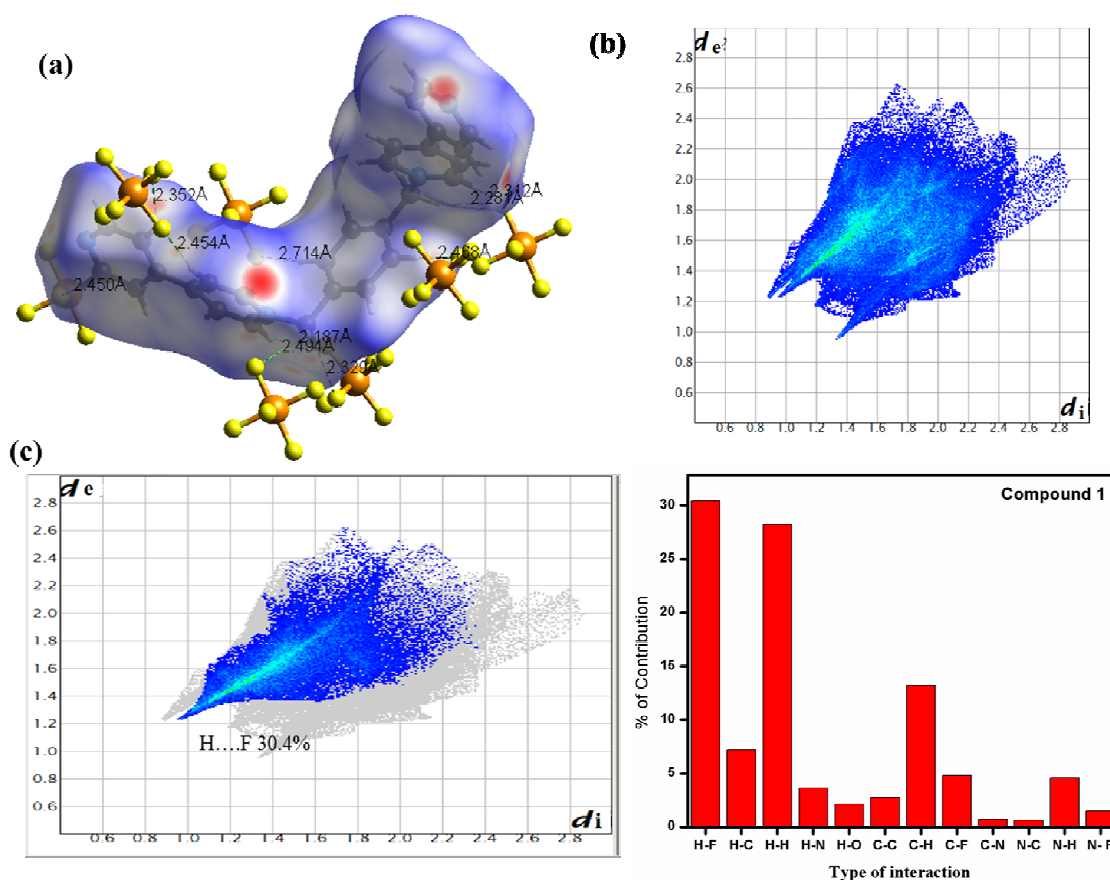


**Figure 8.** Hirshfeld surfaces mapped with (a)  $d_{norm}$  ranging from  $-0.376$  (red) to  $1.441$  (blue), (b) 2D finger print plots with  $d_i$  and  $d_e$  ranging from  $1.0$  to  $2.8$  Å, (c) H...F interactions (left) and percentage contribution of all other interactions around the cation (right) in compound 1 (**1,4-dioxane**).

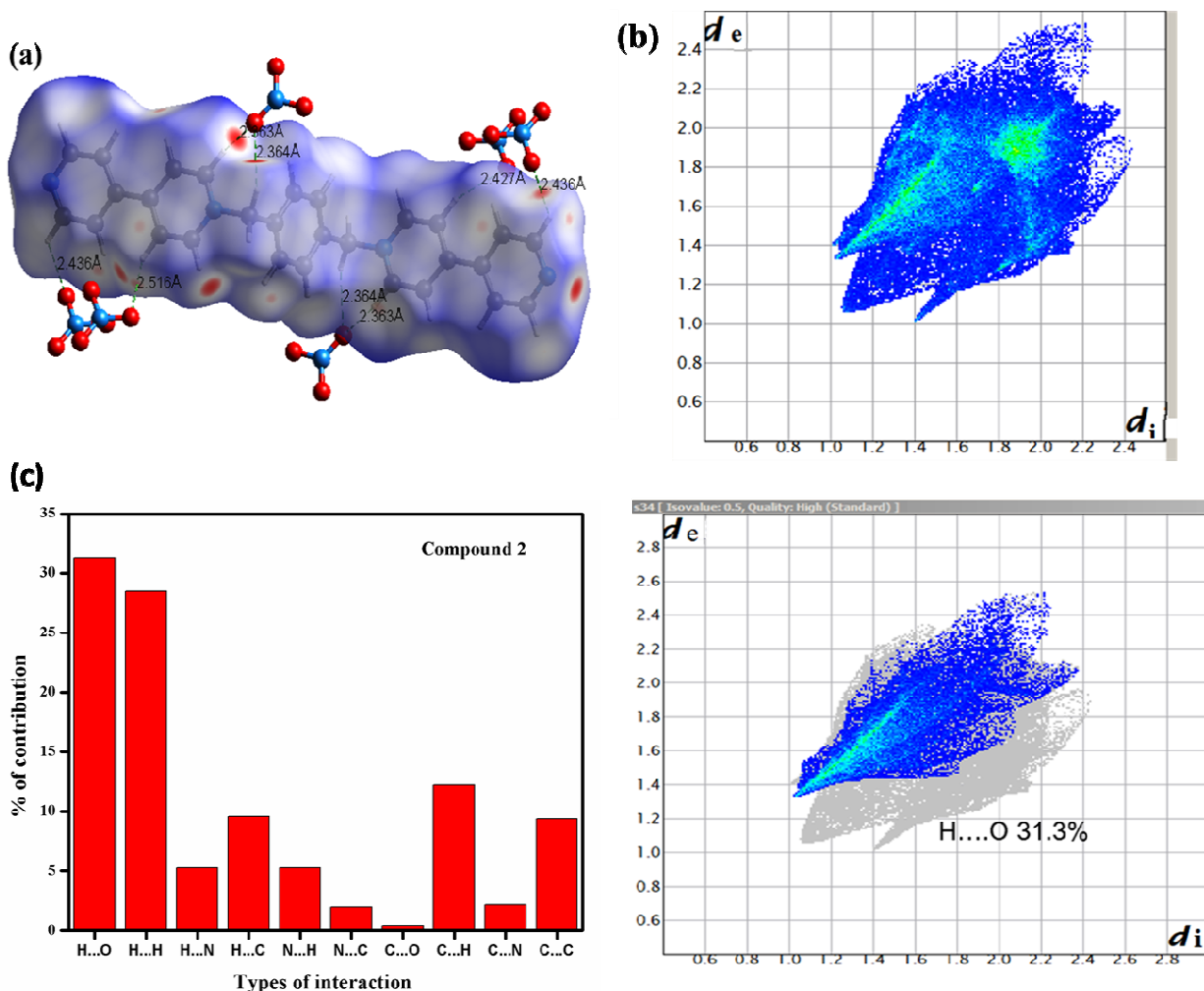


**Figure 9.** Hirshfeld surfaces mapped with (a)  $d_{\text{norm}}$  ranging from  $-0.179$  (red) to  $1.360$  (blue), (b) 2D fingerprint plots with  $d_i$  and  $d_e$  ranging from  $1.0$  to  $2.8$  Å, (c) percentage of contributions from all other interactions around the cation (left) and H...O interactions (right) in compound  $2 \cdot 2\text{H}_2\text{O}$ .

and balanced hydrogen bonding interactions with  $\text{PF}_6^-$  and  $\text{NO}_3^-$  anions in compound  $1 \cdot (1,4\text{-dioxane})$  and compound  $2 \cdot 2\text{H}_2\text{O}$  respectively, that have been mapped over  $d_{\text{norm}}$  ( $-0.3$  to  $1.45$  Å in compound  $1 \cdot (1,4\text{-dioxane})$  and  $-0.1$  to  $1.4$  Å in compound  $2 \cdot 2\text{H}_2\text{O}$  as shown in Figures 8 and 9 respectively (see also Figures S2 and S3 of SI for HSs mapped with the shape index and curvedness). All are the deep red spots, seen in the  $d_{\text{norm}}$  surface, represent the interactions, whereas the blue spots indicate the areas without close contacts. The intensity of the red spots on the Hirshfeld Surfaces of the cationic receptor **c** in compounds  $1 \cdot (1,4\text{-dioxane})$  and  $2 \cdot 2\text{H}_2\text{O}$  clearly indicate that it has been experiencing unbalanced and balanced hydrogen bonding interactions with  $\text{PF}_6^-$  and  $\text{NO}_3^-$  anions respectively (compare Figures 8a and 9a respectively).

1  
2  
3 Among noncovalent contacts, experienced by the cationic receptor **c** in compound  
4  $[\text{C}_{28}\text{H}_{24}\text{N}_4](\text{PF}_6)_2 \cdot (1,4\text{-dioxane})$  (**1**·(**1,4-dioxane**)), the major interactions are  $\text{H}\cdots\text{F}$  (30.4%) and  
5  $\text{H}\cdots\text{H}$  (28.2 %) as shown in Figure 8c (right). The relative contributions from other different  
6 interactions are calculated and given in Figure 8c (left). In the case of  $[\text{C}_{28}\text{H}_{24}\text{N}_4](\text{NO}_3)_2 \cdot 2\text{H}_2\text{O}$   
7 (**2**·**2H<sub>2</sub>O**), and dominating  $\text{H}\cdots\text{O}$  (basically  $\text{C}-\text{H}\cdots\text{O}$  hydrogen bonds) and  $\text{H}\cdots\text{H}$  interactions  
8 are nearly 31.3% and 28.5% respectively among all other interactions as shown in Figure 9c  
9 (left).

10  
11 **Computational studies on different conformers of cationic receptor  $[\text{C}_{28}\text{H}_{24}\text{N}_4]^{2+}$  (**c**),**  
12 **compound  $[\text{C}_{28}\text{H}_{24}\text{N}_4](\text{PF}_6)_2$  (**1**), and compound  $[\text{C}_{28}\text{H}_{24}\text{N}_4](\text{NO}_3)_2$  (**2**).**  
13  
14

15  
16 In continuation of experimental work on cationic receptor **c**, we also performed the theoretical  
17 calculations to find out its conformational structures as such **c** and in compounds **1** and **2**  
18 including the stability of those conformers in gas phase. It is found that its *anti*-conformer ( $E_{\text{elec}}$   
19 =  $-1299.97188$  a.u.) is more stable by  $\sim 1.65$  kcal/mol than its *syn* conformer ( $E_{\text{elec}}$  =  
20  $-1299.96926$  a.u.). The atom numbering is shown to the respective figures to facilitate the  
21 discussion. The conformers of the compounds and the atom numbering are made by GaussView5  
22 software.<sup>36</sup> The x,y,z coordinates of the *anti* and *syn* conformers of the cationic receptor **c** at its  
23 ground state energy minimized structure are given in Table S5 and S6 in the section of  
24 Supporting Information. The structures of the other conformers of **c** around the 1N-24C-52C-  
25 29N dihedral angle are shown in Figure 10. The energy profile diagram corresponding to these  
26 different dihedral angles is shown in Figure 11. The structures of different conformers are  
27 optimized at the interval of  $20^\circ$  dihedral angle. It is found that *anti*-conformer with 1N-24C-52C-  
28 29N dihedral angle of  $-180^\circ$  is the most stable conformer than the other conformers, whereas *syn*  
29 conformer is the least stable conformer. Energy of the intermediate conformers rises very  
30 steeply between,  $-180^\circ$  to  $-240^\circ$  and  $-180^\circ$  to  $-120^\circ$ , 1N-24C-52C-29N dihedral angle,  
31 whereas the steepness of the curve decreases in the both sides, after the above mentioned range  
32 of dihedral angle (cf. Figure 11). Analysis of the energy profile diagram (cf. Figure 11) provides  
33 the energy difference between the most stable and least stable structure, which is  $\sim 3$  kcal/mol.  
34 Thus, this cationic receptor  $[\text{C}_{28}\text{H}_{24}\text{N}_4]^{2+}$  (**c**) is flexible to form ion pair complexes with diverse  
35 anions in a wide range of 1N-24C-52C-29N dihedral angles. We have chosen two different  
36 anions  $\text{PF}_6^-$  and  $\text{NO}_3^-$  in this study to obtain the ion pair compounds  $[\text{C}_{28}\text{H}_{24}\text{N}_4](\text{PF}_6)_2$  (**1**) and  
37  $[\text{C}_{28}\text{H}_{24}\text{N}_4](\text{NO}_3)_2$  (**2**) respectively; the preferable conformations of **c** (cationic receptor) in  
38  
39  
40  
41  
42  
43  
44  
45  
46  
47  
48  
49  
50  
51  
52  
53  
54  
55  
56  
57  
58  
59  
60

presence  $\text{PF}_6^-$  anion (compound **1**) and  $\text{NO}_3^-$  anion (compound **2**) are discussed here. It is found that the compound **2** always prefers to form an *anti*-conformation of **c** with 1N-24C-52C-29N dihedral angle of  $\sim 167^\circ$ . But in the case of compound **1**, both *anti* (with 1N-24C-52C-29N dihedral angle of  $\sim 180^\circ$ ) and *syn* (1N-24C-52C-29N dihedral angle of  $\sim 8^\circ$ ) conformers of **c** are

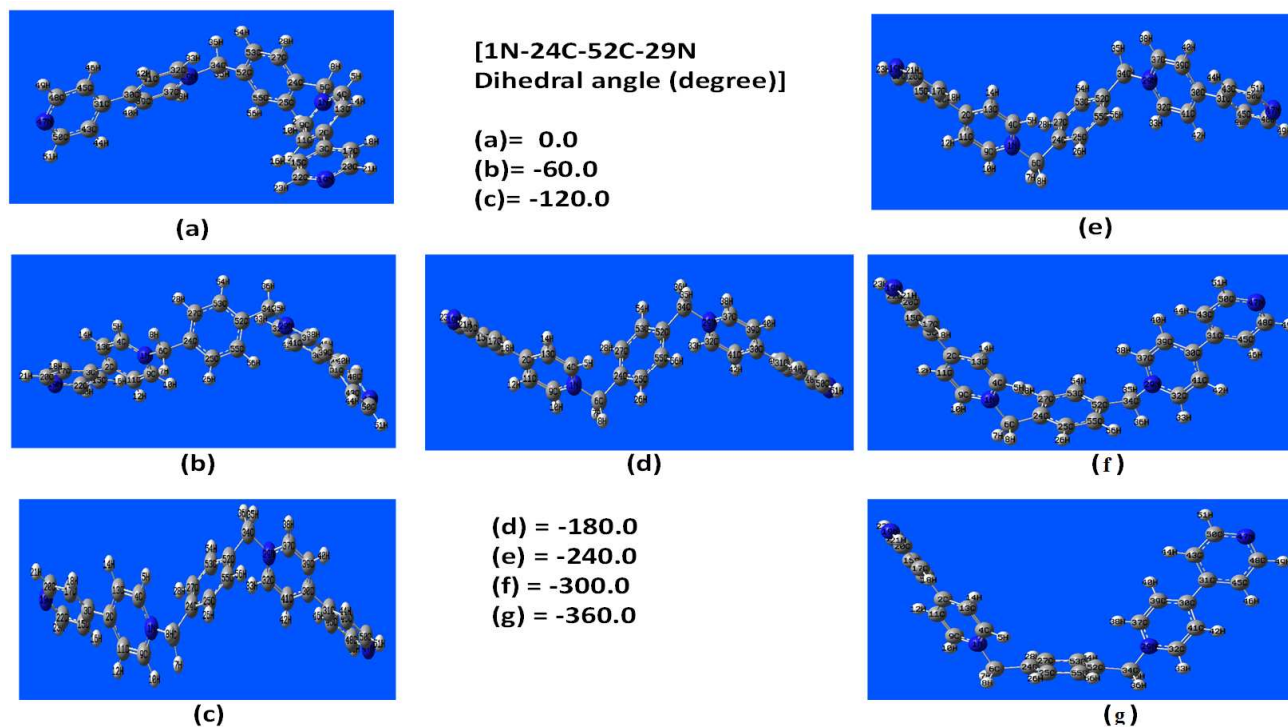


**Figure 10.** Energy minimized structures of different conformers of cationic receptor **c**.

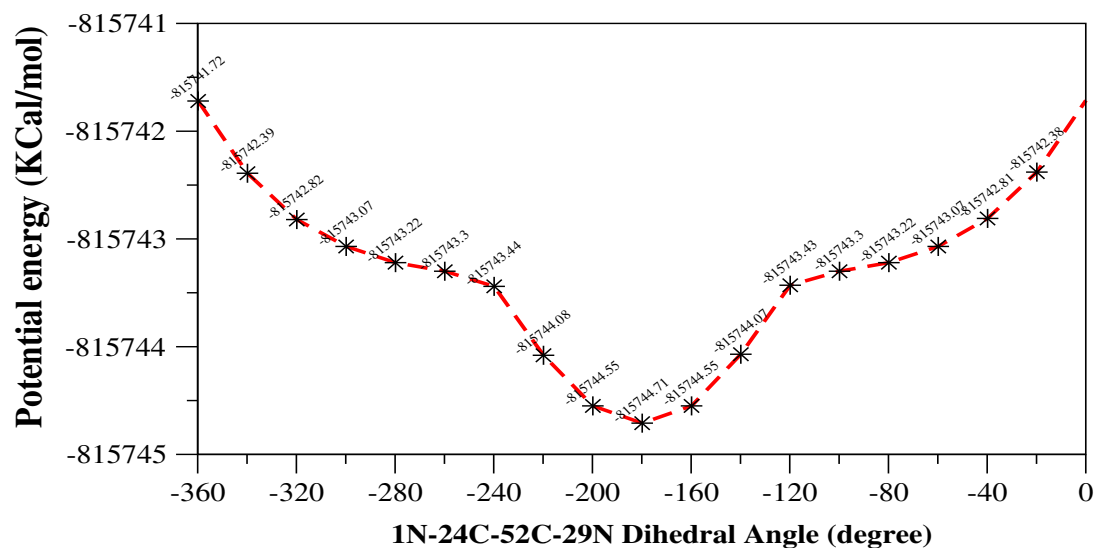


**Figure 11.** Potential energy analysis at different 1N-24C-52C-29N dihedral angles of cationic receptor **c**.

formed with different stabilization energy. The optimized structures of these preferred conformers in compound **2** and in compound **1** with the H-bond indication are shown in panels (a) – (f) of Figure 12. Panel (a) is the *anti* conformer of **c** in compound **2** and panels (b) – (f) are different conformers of **c** in compound **1**. The stabilization energy of the *anti*-conformer of compound **2** is ~229 kcal/mol, whereas the same for the *anti*- and *syn*-conformers of compound **1** are ~215 kcal/mol and ~230 kcal/mol, respectively. Thus, the calculations of

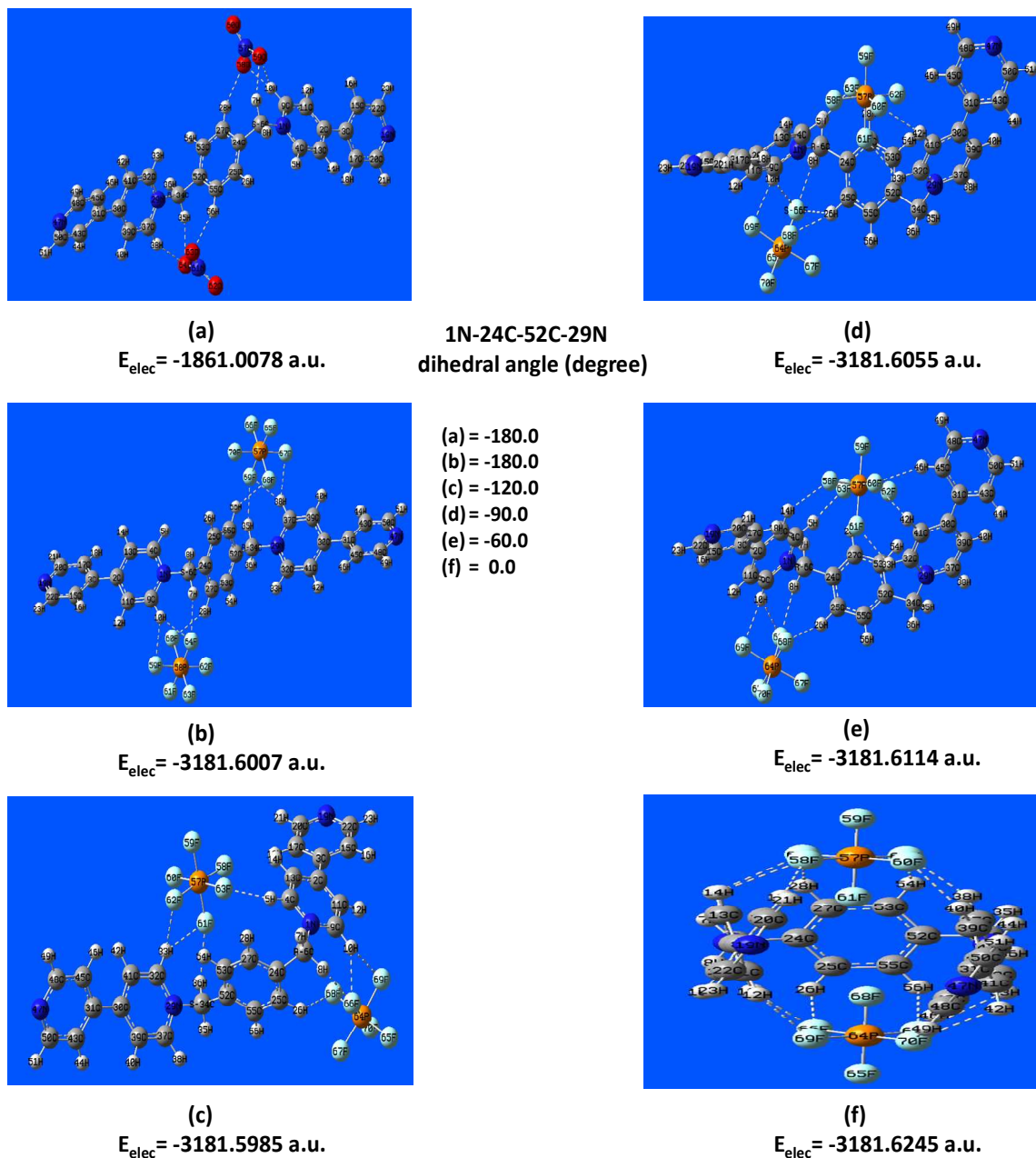


**Figure 12.** Energy minimized structures of *anti*-conformer in compound **2** (panel (a)) and various conformers in compound **1**. (panels (b) – (f)).

Stabilization energy indicate that the *syn* conformer of compound **1**. is more preferable than its *anti*-conformer. The stabilization energies of the intermediate conformers of **c** in compound **1** are also calculated to obtain more detailed conformational analysis of compound **1**.

The calculated stabilization energies of the intermediates with 1N-24C-52C-29N dihedral angles of  $-120^\circ$ ,  $-90^\circ$  and  $-60^\circ$  are  $\sim 214$  kcal/mol,  $\sim 215$  kcal/mol,  $\sim 222$  kcal/mol respectively. The optimized structures of these intermediates with H-bond indication are shown in panels (c), (d) and (e) of Figure 12, respectively. A graphical representation of the stabilization energies of various conformers of **c** in compound **1** with different 1N-24C-52C-29N dihedral angles is shown in Figure 13. It is seen from Figure 13 that the stabilization energy of the

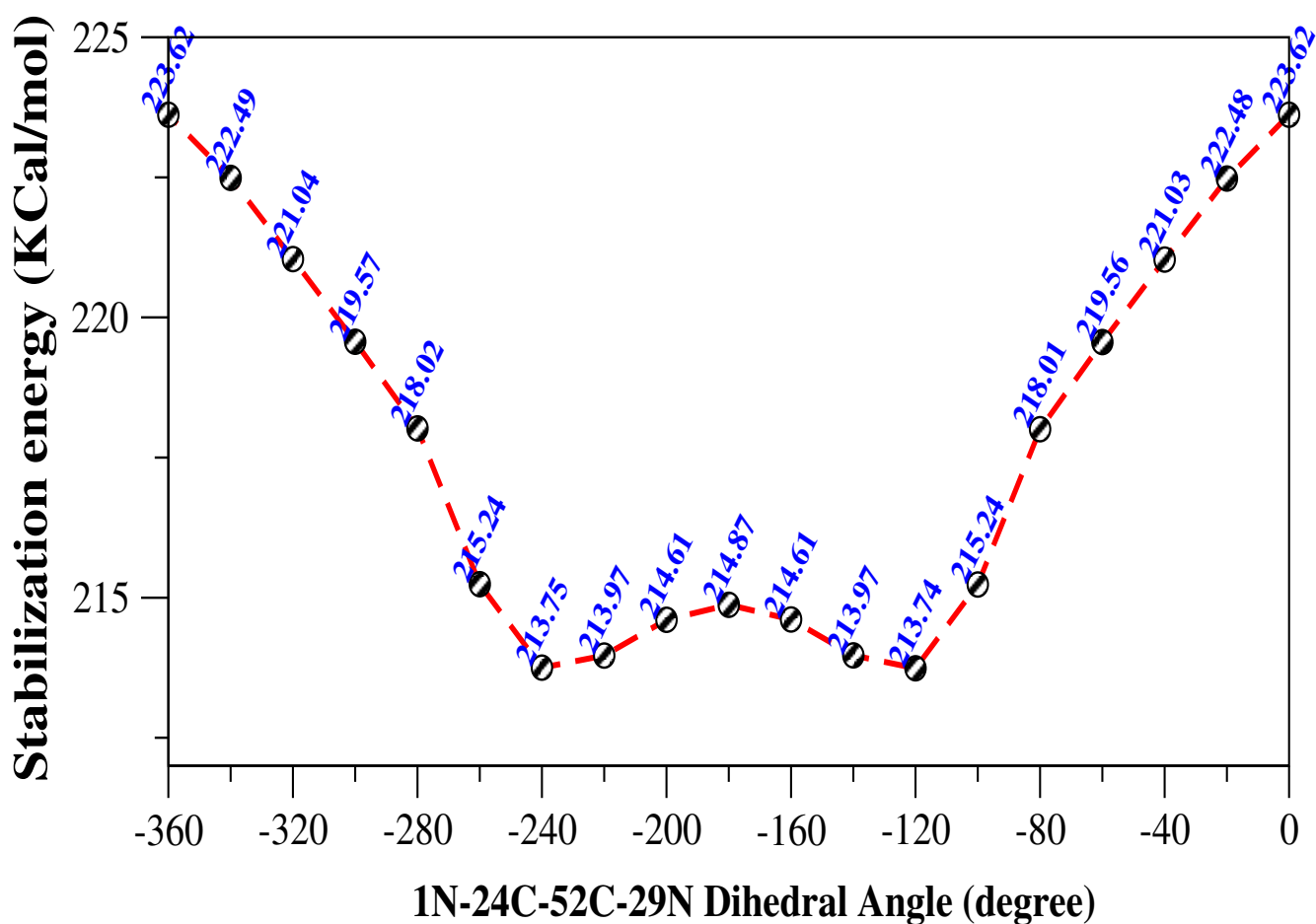


Figure 13. A diagram of stabilization energies at various 1N-24C-52C-29N dihedral angles in **c** in compound **1**.

conformers is decreased in comparison to *anti*-conformer ( $-180^\circ$ ) to  $-120^\circ$  ( $-240^\circ$ ) 1N-24C-52C-29N dihedral angle. Whereas an increment of stabilization energy is observed in different

intermediate conformers in compound **1** in the range of  $-100^\circ$  to  $0^\circ$  1N-24C-52C-29N dihedral angle. It is noted that the stabilization energies of the conformers of Figure 13 should be differed from the actual stabilization energies calculated for  $-180^\circ$ ,  $-120^\circ$ ,  $-90^\circ$ ,  $-60^\circ$  and  $0^\circ$  1N-24C-52C-29N dihedral angles, as the parameter 1N-24C-52C-29N dihedral angle of these conformers (cf. Figure 13) is not optimized. The above discussion on stabilization energies of different conformers of **c** in compound **1** indicates that the energy difference between the different conformers in the  $-100^\circ$  to  $0^\circ$  1N-24C-52C-29N dihedral angle range is a small amount. Thus according to this calculation, the anion  $\text{PF}_6^-$  prefers to form the ion pair complex either with *syn* conformer of **c** or with an intermediate conformer of **c** (cationic receptor). A similar conformation of **c**, found in the crystal structure of **1**·(**1,4-dioxane**), has also been observed in the crystal structure of **c**·**2PF<sub>6</sub>** by Kom-Bei Shiu and co-workers<sup>21</sup> as far as relevant N---C---C---N torsion angles are concerned [ $98.08^\circ$  for **1**·(**1,4-dioxane**) and  $97.28^\circ$  for **c**·**2PF<sub>6</sub>**].

The HOMO and LUMO diagrams of the conformers of cationic receptor **c**, compound **1** and compound **2** are shown in Figure 14 [panels (a) and (b) for cationic receptor **c**; panel (c) for compound **2**; panels (d) and (e) for compound **1**]. Figure 14 shows that the HOMOs of *syn*-cationic receptor as such (Figure 14a), *anti*-cationic receptor as such (Figure 14b), compound **2** (Figure 14c), *anti*-conformer of compound **1** (Figure 14d) and *syn*-conformer of compound **1** (Figure 14e) are stabilized by  $\sim 75$ ,  $\sim 73$ ,  $\sim 47$ ,  $\sim 95$  and  $\sim 97$  kcal/mol, respectively compared to their respective LUMOs. These data indicate that the HOMO-LUMO stabilization is increased during the ion pair complex formation of cationic receptor (**c**) with  $\text{PF}_6^-$  anion, whereas the same is decreased during the ion pair complex formation of cationic receptor (**c**) with  $\text{NO}_3^-$  anion.

**Natural bond orbital (NBO) analysis.** In order to have more insight into the stabilization of compounds **1** and **2** with respect to the conformations of receptor cation **c**, we performed the NBO analysis of the different conformers of these compounds. The results of the donor-acceptor interactions of different conformers of compound **1** and compound **2** are given in Table 6. The donor orbital (*i*), acceptor orbital (*j*), calculated second-order interaction energies between the donor-acceptor orbitals [ $E^2(i,j)$ ] and H-bond distances in compound **2** and that in different conformers of compound **1** are given in this table. NBO analysis of compound **2** indicates that  $\sim 60$  kcal/mol stabilization energy is acquired due to the H-bond formation between the oxygen (O) lone pairs (LP) and  $\sigma^*$  C-H bonds. It is found that both the  $\text{NO}_3^-$  anions interact symmetrically through H-bonds with the two bipyridine sides of the cationic receptor **c** (Figure

12a; see also Figure 7b, the experimental crystallographic evidence). That is why, **c** in compound **2** prefers *anti* conformation. A minute inspection of the Figure 12a and its NBO analysis indicate that the H-bond interaction between LP of 64 O and  $\sigma^*$  of 37C–38H on the

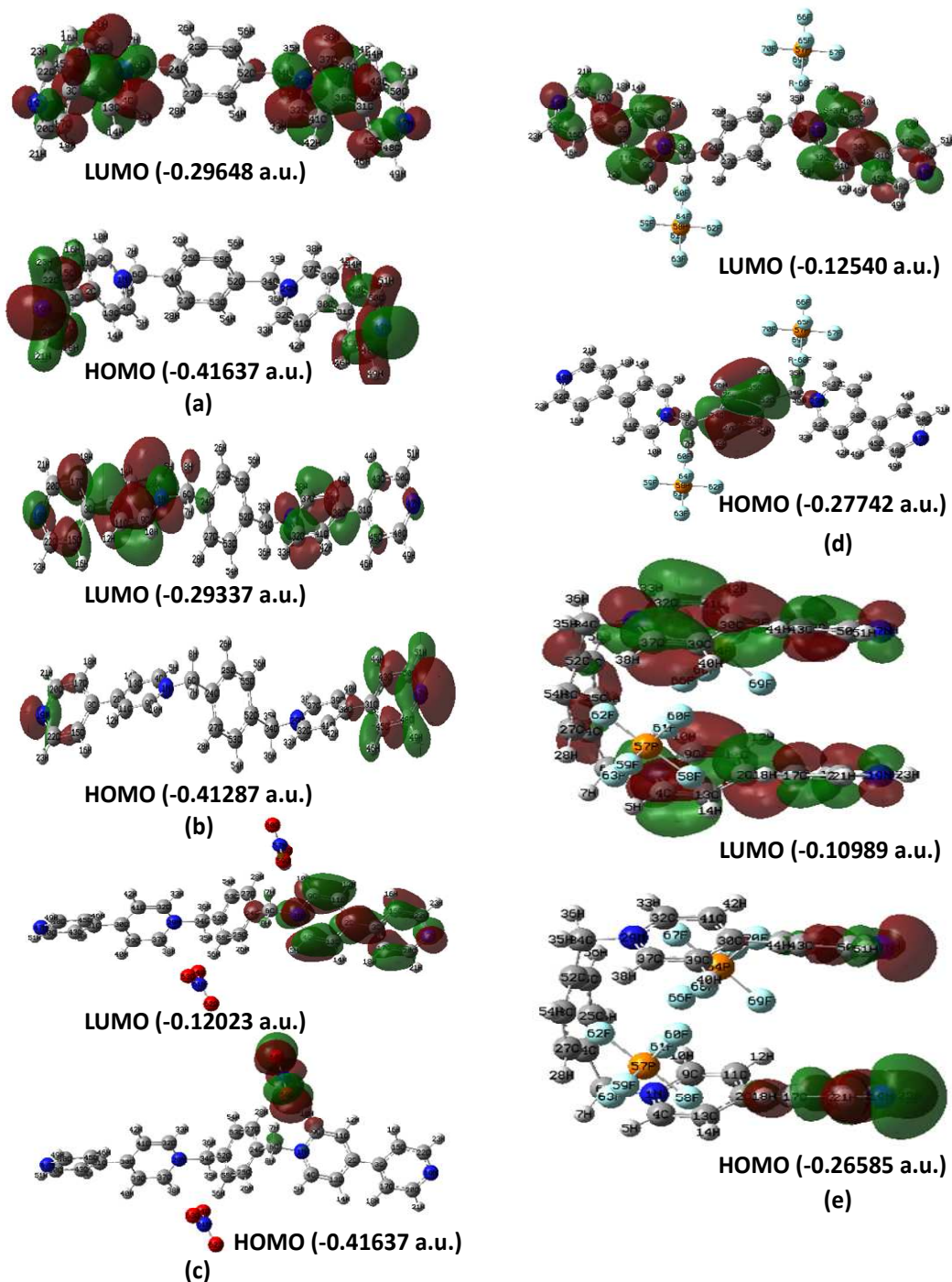


**Figure 14.** HOMO-LUMO diagrams of (a) syn- conformer of cationic receptor, (b) anti- conformer of cationic receptor, (c) anti- conformer of compound **2**, (d) anti- conformer of compound **1** and (e) syn- conformer of compound **1**.

one bipyridine side of the cationic receptor (**c**) stabilizes the compound **2** by  $\sim 14$  kcal/mol with 1.943 Å H-bond distance. On the other hand, H-bond between LP of 58 O and  $\sigma^*$  of 9C–10H on the other bipyridine side of the cationic receptor (**c**) gives the compound **2** more stability by  $\sim 21$  kcal/mol with 1.833 Å H-bond distance. These two marginally different symmetric H-bonding interactions of the two opposite bipyridine sides of the cationic receptor (**c**) makes the compound **2** somewhat different orientation from the actual *anti*-conformation. Thus, the compound **2** prefers a predominantly *anti*-orientation with 1N-24C-52C-29N dihedral angle of  $\sim 167^\circ$  (not exactly  $180^\circ$ ) as shown in Figure 12a. On the other hand, the different conformational orientations with 1N-24C-52C-29N dihedral angles of  $-180^\circ$ ,  $-120^\circ$ ,  $-90^\circ$ ,  $-60^\circ$  and  $-8^\circ$  of compound **1** show  $\sim 22$ ,  $\sim 26$ ,  $\sim 32$ ,  $\sim 36$  and  $\sim 32$  kcal/mol stability, respectively, on H-bonding interactions between the LPs of different F atoms and different  $\sigma^*$  C–H bonds in compound **1**. Therefore, this result (consistent with energy minimized calculations, *vide supra*) also suggests that  $\text{PF}_6^-$  anion prefers to form an ion pair complex either with intermediate ( $-90^\circ$ ,  $-60^\circ$ ) or *syn* orientation ( $-8^\circ$ ) of the cationic receptor **c**. A symmetric H-bond formation around **c** with respect to its two bipyridine sides is observed (Figure 12b). This can be also encountered from the data given in Table 6. The H-bonding interaction between the LP of 64F and  $\sigma^*$  9C–10H bond on the one bipyridine side and the H-bond between LP of 69F  $\sigma^*$  37C–38H bond on the other bipyridine side provide similar  $\sim 6$  kcal/mol of stabilization. Similarly, the LP of 59F and  $\sigma^*$  9C–10H bond on the one bipyridine side and the LP of 67F  $\sigma^*$  37C–38H bond on the other bipyridine side provide similar  $\sim 3$  kcal/mol of stabilization. These symmetric H-bonding interactions give the proper *anti*-orientation conformer of compound **1** as shown in Figure 12b. This type of symmetric H-bonding interactions are absent in other conformers of compound **1** as shown in Figures 12c, 12d and 12e. In the case of *syn* conformer of compound **1** (Figure 12f), an unbalanced symmetric H-bonding interaction is observed between the LP of 62 F and  $\sigma^*$  of 37C–38H bond and LP of 66 F and  $\sigma^*$  of 9C–10H bond. Both the H-bonding interaction stabilize the molecule by  $\sim 5$  kcal/mol and has the bond distance of 2.18 Å. The same is observed in the H-bond, initiated by LPs of 58F, 70F, 60F and 69F atoms. These are the forces behind the stability and *syn* orientation of the conformer of compound **1** (Figure 12f). The NBO analysis shows that the overall H-bonding stability is highest in the conformer of compound **1** with the 1N-24C-52C-29N dihedral of  $-60^\circ$ , an intermediate one (not  $-8^\circ$ , *syn* conformer). Thus, this study also indicates that  $\text{PF}_6^-$  anion prefers to form an unusual intermediate conformation of **c** or its

1  
2  
3 *syn* conformation, whereas  $\text{NO}_3^-$  anion prefers to form normal *anti* conformation of **c**, cationic  
4  
5 receptor.

6  
7 In order to validate the above discussion, we performed the equilibrium constant  
8  
9 calculations between different conformers of cationic receptor **c** and the compound **1**. The  
10  
11 calculated values of equilibrium constant at different temperature (T, Kelvin) are given in Table  
12  
13 7. It is found that *anti* conformer of cationic receptor **c** is dominant than *syn* conformer of it at  
14  
15 the equilibrium in the temperature range of 100-800 K. The percentage of *syn* conformer is  
16  
17 increased with the temperature. The *syn* conformer of cationic receptor **c** occupies only 1.16% at  
18  
19 the room temperature (300K). Similar analysis of the conformers of compound **1** shows that *syn*  
20  
21 conformer is dominant than *anti* conformer at their equilibrium at different temperatures (Table  
22  
23 7). Even at room temperature (300K), the conversion of *syn* to *anti* is not expected to be  
24  
25 achievable. An increment of this conversion is observed from 650 K temperature. So it is  
26  
27 expected that the barrier of *syn-anti* conversion of compound **1** can be overcome at higher  
28  
29 temperature. Similar analysis of two intermediate conformers with 1N-24C-52C-29N dihedral  
30  
31 angle of  $-90^\circ$  and  $-60^\circ$  indicates that these two conformers are dominant than *anti*-conformer of  
32  
33 compound **1** in the respective equilibrium. The increment of this conversion with temperature is  
34  
35 higher than the *syn-anti* conversion of compound **1**. An opposite scenario is observed  
36  
37 considering the intermediate conformer with 1N-24C-52C-29N dihedral angle of  $-120^\circ$  and *anti*-  
38  
39 conformer equilibrium of compound **1**. In this case, *anti*-conformer is found as a dominant in the  
40  
41 equilibrium. So the calculations of equilibrium constant between different conformers of  
42  
43 compound **1** also suggest that the  $\text{PF}_6^-$  anion prefers to form complex with cationic receptor **c** at  
44  
45 its *syn* or intermediate ( $-90^\circ$  and  $-60^\circ$ ) orientations.

#### 46 ■ SUMMARY

47 An organic receptor, 1,1''-1,4-phenylene-bis(methylene)bis-4,4'-bipyridinium cation  
48  
49  $[\text{C}_{28}\text{H}_{24}\text{N}_4]^{2+}$  (**c**) was known to be isolated as its *anti*- as well as its *syn*-conformations. In the  
50  
51 present work, we have isolated this cationic receptor as an unusual intermediate conformation  
52  
53 (neither *syn* nor *anti*) with  $\text{PF}_6^-$  anion in compound  $[\text{C}_{28}\text{H}_{24}\text{N}_4](\text{PF}_6)_2 \cdot (1,4\text{-dioxane})$  (**1**·(**1,4-**  
54  
55 **dioxane**)). The energetically favored *anti* conformation of this organic cation has been described  
56  
57 in its nitrate salt  $[\text{C}_{28}\text{H}_{24}\text{N}_4](\text{NO}_3)_2 \cdot 2\text{H}_2\text{O}$  (**2**·**2H<sub>2</sub>O**). Both compounds are characterized by single  
58  
59 crystal X-ray crystallography. We have a given rationale of why an atypical intermediate  
60  
61 conformer of the title receptor is stabilized with  $\text{PF}_6^-$  anion and a typical *anti*-form of this

receptor is isolated with nitrate anion, with the help of supramolecular hydrogen bonding interactions and Hirshfeld surface analysis.

A detailed theoretical account of the stability of the various conformers of the cationic receptor  $[C_{28}H_{24}N_4]^{2+}$  (**c**), compound  $[C_{28}H_{24}N_4](PF_6)_2$  (**1**) and compound  $[C_{28}H_{24}N_4](NO_3)_2$  (**2**) has been discussed in this study by calculating their electronic stability, HOMO–LUMO stabilization and NBO analysis. Final conclusion of their stability is obtained by calculation of conformational equilibrium constants at different temperatures between the conformers of the cationic receptor **c** and compound **1**. It is found that *anti* form of the cationic receptor **c** is more stable than its *syn* orientation, whereas, in presence of  $PF_6^-$  anion, it prefers *syn* or an intermediate (with 1N-24C-52C-29N dihedral angles of  $-60^\circ$  and  $-90^\circ$ ) conformers. An opposite scenario of usual *anti* orientation of the cationic receptor **c** with little deviation is observed, when the cationic receptor **c** binds with  $NO_3^-$  anion. A symmetric interaction through H-bonds between the two bipyridine sides of the cationic receptor **c** and two  $NO_3^-$  anions is the main cause behind the *anti*-orientation of the compound **2**, whereas, an unbalanced symmetric H-bonding interactions between the LP of F atoms ( $PF_6^-$  anion) and  $\sigma^*$  of C-H bonds (cationic receptor **c**) give the compound **2** unusual *syn* or intermediate orientation.

## ■ ASSOCIATED CONTENT

### Supporting Information

Elemental analyses plots; Hirshfeld Surface Analysis plots; First lowest thirty four vibrational frequencies (in  $cm^{-1}$ ) of the optimized structures of *anti* and *syn* cationic receptor **c** conformers and different conformers of compound **2** (in a tabular form); Rotational constant values (A, B, C in GHz) and symmetry numbers for different conformers of 2-butene, cationic receptor **c** and compound **1** (in a tabular form); rotational ( $q^{rot}$ ) and vibrational ( $q^{vib}$ ) partition functions values of different conformers of 2-butene, cationic receptor **c** and compound **1** at different temperature (in a tabular form); calculated and experimental equilibrium constants (K) at different temperatures (in kelvin) between cis-2-butene and trans-2-butene (in a tabular form). The x, y, z coordinates of the ground state energy minimized structure of the different conformers of the cationic receptor **c**, compound **1** and compound **2** are also given in Tables S5-S9, in the supporting information. The conformational analysis of the cationic receptor **c** and compound **1** with respect to benzene torsional angle are also discussed in the Supporting information. CCDC 1525549 and CCDC

1  
2  
3 1023590 contains the supplementary crystallographic data for compounds **1**·(**1,4-dioxane**) and  
4 **2**·**2H<sub>2</sub>O** respectively. Relevant crystal data can be obtained free of charge via  
5 <http://www.ccdc.cam.ac.uk/conts/retrieving.html>, or from the Cambridge Crystallographic Data  
6 Centre, 12 Union Road, Cambridge CB2 1EZ, UK; fax: (+44) 1223-336-033; or e-mail:  
7 [deposit@ccdc.cam.ac.uk](mailto:deposit@ccdc.cam.ac.uk).  
8  
9  
10  
11  
12  
13

#### 14 ■ AUTHOR INFORMATION

15 Corresponding Author

16 \*Phone +91-40 – 2313-4853; email [skdas@uohyd.ac.in](mailto:skdas@uohyd.ac.in) (SKD)

#### 17 Notes

18 The authors declare no competing financial interest.  
19  
20  
21  
22  
23  
24  
25

#### 26 ■ ACKNOWLEDGMENTS

27 We thank SERB, DST, Government of India, for financial support (Project No. SB/S1/IC-  
28 34/2013). We are grateful to UGC, New Delhi, for UPE-II grant. R.S. acknowledges UGC, New  
29 Delhi, India, for his doctoral fellowship. Our special thanks to Professor S. Mahapatra, School of  
30 Chemistry, University of Hyderabad for his help in theoretical calculations and CMSD for  
31 computational facility.  
32  
33  
34  
35  
36  
37  
38

#### 39 ■ REFERENCES

- 40  
41  
42 (1) Klärner, F.-G.; Kahlert, B. Molecular Tweezers and Clips as Synthetic Receptors.  
43 Molecular Recognition and Dynamics in Receptor–Substrate Complexes. *Acc. Chem. Res.* **2003**,  
44 *36*, 919-932.  
45 (2) Lehn, J. – M. *Supramolecular Chemistry. Concepts and Perspectives*, VCH, Weinheim,  
46 **1995**.  
47 (3) Gallivan, J. P.; Dougherty, D. A. A Computational Study of Cation– $\pi$  Interactions vs Salt  
48 Bridges in Aqueous Media: Implications for Protein Engineering. *J. Am. Chem. Soc.* **2000**, *122*,  
49 870-874.  
50 (4) Prins, L. J.; Reinhoudt, D. N.; Timmerman, P. Noncovalent Synthesis Using Hydrogen  
51 Bonding. *Angew. Chem. Int. Ed.* **2001**, *40*, 2382-2426.  
52 (5) Sinnokrot, M. O.; Valeev, E. F.; Sherrill, C. D. Estimates of the Ab Initio Limit for  $\pi$ – $\pi$   
53 Interactions: the Benzene Dimer. *J. Am. Chem. Soc.* **2002**, *124*, 10887-10893.  
54  
55  
56  
57  
58  
59  
60

- 1  
2  
3  
4  
5  
6  
7  
8  
9  
10  
11  
12  
13  
14  
15  
16  
17  
18  
19  
20  
21  
22  
23  
24  
25  
26  
27  
28  
29  
30  
31  
32  
33  
34  
35  
36  
37  
38  
39  
40  
41  
42  
43  
44  
45  
46  
47  
48  
49  
50  
51  
52  
53  
54  
55  
56  
57  
58  
59  
60
- (6) Sokolov, A. N.; Friščić, T.; MacGillivray, L. R. Enforced Face-to-Face Stacking of Organic Semiconductor Building Blocks within Hydrogen-Bonded Molecular Cocrystals. *J. Am. Chem. Soc.* **2006**, *128*, 2806-2807.
- (7) Nohra, B.; Graule, S.; Lescop, C.; Réau, R. Mimicking [2,2]-Paracyclophane Topology: Molecular Clips for the Coordination-Driven Cofacial Assembly of  $\pi$ -Conjugated systems. *J. Am. Chem. Soc.* **2006**, *128*, 3520-3521.
- (8) Meyer, E. A.; Castellano, R. K.; Diederich, F. Interactions with Aromatic Rings in Chemical and Biological Recognition. *Angew. Chem. Int. Ed.* **2003**, *42*, 1210-1250.
- (9) Neelakandan, P. P.; Hariharan, M.; Ramaiah, D. Synthesis of a Novel Cyclic Donor-Acceptor Conjugate for Selective Recognition of ATP. *Org. Lett.* **2005**, *7*, 5765-5768.
- (10) Kim, E.-i.; Paliwal, S.; Wilcox, C. S. Measurements of Molecular Electrostatic Field Effects in Edge-to-Face Aromatic Interactions and CH- $\pi$  Interactions with Implications for Protein Folding and Molecular Recognition. *J. Am. Chem. Soc.* **1998**, *120*, 11192-11193.
- (11) Fráusto da Silva, J. J. R.; Williams, R. J. P. *The Biological Chemistry of the Elements, the Inorganic Chemistry of Life*, Oxford University Press, Oxford, **1991**, Chapter 10.
- (12) Philp, D.; Stoddart, J. F. Self-Assembly in Natural and Unnatural Systems. *Angew. Chem. Int. Ed. Engl.* **1996**, *35*, 1154-1196.
- (13) Rekharsky, M. V.; Inoue, Y. Complexation Thermodynamics of Cyclodextrins. *Chem. Rev.* **1998**, *98*, 1875-1918.
- (14) Collet, A.; Dutasta, J. P.; Lozach, B.; Canceill, J. Cyclotrimeratrylenes and Cryptophanes : Their Synthesis and Applications to Host-Guest Chemistry and to the Design of New Materials. *Top. Curr. Chem.* **1993**, *165*, 103-129.
- (15) Lee, J. W.; Samal, S.; Selvapalam, N.; Kim, H. J.; Kim, K. Cucurbituril Homologues and Derivatives: New Opportunities in Supramolecular Chemistry. *Acc. Chem. Res.* **2003**, *36*, 621-630.
- (16) Warmuth, R.; Yoon, J. Recent Highlights in Hemicarcerand Chemistry. *Acc. Chem. Res.* **2001**, *34*, 95-105.
- (17) Corbellini, F.; Mulder, A.; Sartori, A.; Ludden, M. J. W.; Casnati, A.; Ungaro, R.; Huskens, J.; Crego-Calama, M.; Reinhoudt, D. N. Assembly of a Supramolecular Capsule on a Molecular Printboard. *J. Am. Chem. Soc.* **2004**, *126*, 17050-17058.
- (18) Harmata, M. In *Encyclopedia of Supramolecular Chemistry, Molecular Clefts and Tweezers*, Atwood, J. L.; Steed, J. W. Marcel Dekker, Eds. New York, **1997**, Vol. 2, pp 887-900.
- (19) Klärner, F.-G.; Panitzky, J.; Bläser, D.; Boese, R. Synthesis and Supramolecular Structures of Molecular Clips. *Tetrahedron.* **2001**, *57*, 3673-3687.
- (20) Fyfe, M. C. T.; Stoddart, J. F.; White, A. J. P.; Williams, D. J. Novel Clay-Like and Helical Superstructures Generated using Arene-Arene Interactions. *New. J. Chem.* **1998**, 155-157.
- (21) Liu, S.-A.; Kuo, T.-S.; Lee, G.-H.; Shiu, K.-B. Sensitivity in Supramolecular Architectures of Polyaromatic Salts Containing Two Singly-Pimerized Bipyridines. *J. Chin. Chem. Soc. (Taipei)* **2007**, *54*, 607-611.
- (22) Bruker. SADABS, SMART, SAINT and SHELXTL, Bruker AXS Inc., Madison, Wisconsin, USA, **2000**.
- (23) Sheldrick, G.M.; SHELX-97, Program for Crystal Structure Solution and Analysis, University of Gottingen, Gottingen, Germany, **1997**.
- (24) Frisch, M. J.; Trucks, G. W.; Schlegel, H. B.; Scuseria, G. E.; Robb, M. A.; Cheeseman, J. R.; Scalmani, G.; Barone, V.; Mennucci, B.; Petersson, G. A. *et al.* Gaussian 09, Revision B.01; Gaussian, Inc.: Wallingford, CT, **2010**.

- 1  
2  
3 (25) Li, P.; Bu, Y.; Ai, H. Density Functional Studies on Conformational Behaviors of  
4 Glycinamide in Solution. *J. Phys. Chem. B.* **2004**, *108*, 1405-1413.
- 5 (26) Li, H.-Y.; Pu, M.; Liu, K.-H.; Zhang, B.-F.; Chen, B.-H. A Density-Functional Theory  
6 Study on Double-Bond Isomerization of 1-Butene to Cis-2-Butene Catalyzed by Zeolites. *Chem.*  
7 *Phys. Lett.* **2005**, *404*, 384-388.
- 8 (27) Justino, L. L. G.; Ramos, M. L.; Abreu, P. E.; Carvalho, R. A.; Sobral, A. J. F. N.; Scherf,  
9 U.; Burrows, H. D. Conformational Studies of Poly(9,9-dialkylfluorene)s in Solution Using  
10 NMR Spectroscopy and Density Functional Theory Calculations. *J. Phys. Chem. B.* **2009**, *113*,  
11 11808-11821.
- 12 (28) Haghdad, M.; Farokhi, N. Density Functional Theory(DFT) Calculations of  
13 Conformational Energies and Interconversion Pathways in 1, 2, 7-Thiadiazepane. *J. Serb. Chem.*  
14 *Soc.* **2011**, *76*, 395-406.
- 15 (29) Szczepaniak, M.; Moc, J. Conformational Studies of Gas-Phase Ribose and 2-Deoxyribose  
16 by Density Functional, Second Order PT and Multi-Level Method Calculations: the Pyranoses,  
17 Furanoses, and Open-Chain Structures. *Carbohydrate Research.* **2014**, *384*, 20-36.
- 18 (30) Happel, J.; Hnatow, M. A.; Mezaki, R. Isomerization Equilibrium Constants of n-Butanes.  
19 *J. Chem. Eng. Data* **1971**, *16*, 206-209.
- 20 (31) Madhu, V.; Sabbani, S.; Kishore, R.; Naik, I. K.; Das, S. K. Mechanical Motion in the Solid  
21 State and Molecular Recognition: Reversible Cis–Trans Transformation of an Organic Receptor  
22 in a Solid–Liquid Crystalline State Reaction Triggered by Anion Exchange. *CrystEngComm.*  
23 **2015**, *17*, 3219-3223.
- 24 (32) Brouwer, E. B.; Udachin, K. A.; Enright, G. D.; Ripmeester, J. A. Amine Guest Size and  
25 Hydrogen-Bonding Influence the Structures of -Butylcalix[4]arene Inclusions. *Chem. Commun.*  
26 **2000**, 1905-1906.
- 27 (33) Wolff. S. K.; Grimwood. D. J.; McKinnon. J. J.; Turner. M. J.; Jayatilaka. D.; and  
28 Spackman. M. A. Crystal Explorer 3.1 (**2013**), University of Western Australia, Crawley,  
29 Western, Australia, **2005–2013**, <http://hirshfeldsurface.net/CrystalExplorer>.
- 30 (34) Soman. R.; Sujatha. S.; and Arunkumar. C. Quantitative Crystal Structure Analysis of  
31 Fluorinated Porphyrins. *J. Fluorine Chem.* **2014**, *163*, 16-22.
- 32 (35) Titi. H. M.; Patra. R.; and Goldberg. I. Exploring Supramolecular Self-Assembly of  
33 Tetraarylporphyrins by Halogen Bonding: Crystal Engineering with Diversely Functionalized  
34 Six-Coordinate Tin(L)2–Porphyrin Tectons. *Chem. Eur. J.* **2013**, *19*, 14941-14949.
- 35 (36) GaussView, Version 5, Dennington, Roy; Keith, Todd; Millam, John. Semichem Inc.,  
36 Shawnee Mission, KS, **2009**.
- 37  
38  
39  
40  
41  
42  
43  
44  
45  
46  
47  
48  
49  
50  
51  
52  
53  
54  
55  
56  
57  
58  
59  
60

**Table 1.** Crystallographic data and structure refinement for compound **1.(1,4-dioxane)** and **2.2H<sub>2</sub>O**

	<b>1.(1,4-dioxane)</b>	<b>2·2H<sub>2</sub>O</b>
Empirical formula	C <sub>32</sub> H <sub>32</sub> F <sub>12</sub> N <sub>4</sub> O <sub>2</sub> P <sub>2</sub>	C <sub>28</sub> H <sub>28</sub> N <sub>6</sub> O <sub>8</sub>
Formula weight	794.56	576.56
Temperature (K)	100(2) K	298 K
Crystal size (mm)	0.20x0.16x0.06	0.21x0.17x0.14
Crystal system	Triclinic	Monoclinic
space group	P-1	p21/n
Z	2	2
Wavelength(A)	0.71073	0.71073
Unit cell dimensions		
a [Å]	9.2462(7)	4.5103(9)
b [Å]	11.7988(9)	19.774(4)
c [Å]	16.7537(13)	15.054(3)
α [°]	106.49(10)	90
β [°]	103.76(10)	97.786(4)
γ [°]	98.33(10)	90
Volume [Å <sup>3</sup> ]	1657.3(2)	1331.2(5)
Calculated density (Mg/m <sup>-3</sup> )	1.592	1.428
Reflections collected/ unique	15442/4749	15147/3145
R(int)	0.0408	0.0604
F(000)	812	604
Max. and min. antission	0.985 and 0.954	0.956 and 0.989
Theta range for data collection (deg.)	1.33 to 25.07	0.956 to 28.23
Refinement method	Full-matrix least-square on F <sup>2</sup>	Full-matrix least-square on F <sup>2</sup>
Data/restrains/parameters	5829/0/469	3145/0/190
Goodness-of-fit on F <sup>2</sup>	1.198	1.003
R <sub>1</sub> /wR <sub>2</sub> [I>2sigma(I)]	0.0713/0.1378	0.0915/0/0.264
R <sub>1</sub> /WR <sub>2</sub> (all data)	0.0900/0.1452	0.142/0.304

Largest diff. peak and hole      0.501 and -0.270 e.Å<sup>-3</sup>      0.487 and -0.284 e.Å<sup>-3</sup>

**Table 2.** Complete list of bond lengths [Å] and angles [deg] for C<sub>28</sub>H<sub>24</sub>N<sub>4</sub>[(PF<sub>6</sub>)<sub>2</sub>·(1,4-dioxane) (1·(1,4-dioxane))

C(7)-N(3)	1.474(5)	C(18)-N(1)	1.347(4)
C(8)-N(3)	1.343(5)	C(26)-N(2)	1.333(5)
C(9)-C(10)	1.393(5)	C(29)-C(30)#1	1.492(6)
C(11)-C(12)	1.361(5)	C(32)-C(31)#2	1.485(6)
C(13)-C(17)	1.193(5)	F(1)-P(1)	1.594(2)
O(1)-C(29)-C(30)#1	109.8(3)	F(4)-P(1)-F(2)	179.85(18)
O(2)-C(31)-C(32)#2	111.3(3)	F(7)-P(2)-F(9)	89.71(13)
C(23)-N(1)-C(19)	120.6(3)	N(2)-C(26)-C(25)	123.8(4)
C(19)-N(1)-C(18)	118.2(3)	N(4)-C(16)-C(17)	125.0(4)
C(30)-O(1)-C(29)	108.7(3)	N(1)-C(23)-C(22)	121.6(3)

Symmetry antiformations used to generate equivalent atoms#1-x+2,-y+1,-z #2 -x+1,-y+1,-z+2

**Table 3.** Hydrogen bonds for compound 1·(1,4-dioxane) [ Å and °].

D-H...A	d(D-H)	d(H...A)	d(D...A)	<(DHA)
C(22)-H(22)...N(4)#3	0.95	2.42	3.308(5)	155.9
C(28)-H(28)...N(4)#3	0.95	2.65	3.482(5)	146.3
C(9)-H(9)...N(2)#4	0.95	2.42	3.302(5)	154.0
C(8)-H(8)...F(1)#5	0.95	2.30	3.156(4)	149.4
C(7)-H(7A)...F(6)#5	0.99	2.42	3.411(4)	178.2
C(7)-H(7B)...F(7)#6	0.99	2.54	3.422(4)	149.1
C(2)-H(2)...F(6)#7	0.95	2.59	3.509(4)	161.7
C(23)-H(23)...F(9)#8	0.95	2.43	3.286(4)	150.5
C(18)-H(18A)...F(9)#8	0.99	2.37	3.304(4)	157.8
C(11)-H(11)...F(3)	0.95	2.58	3.524(4)	170.3

C(17)-H(17)...F(5)	0.95	2.46	3.266(4)	143.0
C(15)-H(15)...F(12)#9	0.95	2.58	3.501(4)	164.0

Symmetry antiformations used to generate equivalent atoms:

#3  $x-1, y, z-1$  #4  $x+1, y+1, z+1$  #5  $x, y+1, z$  #6  $-x, -y+1, -z+1$  #7  $-x, -y+1, -z$  #8  $x, y+1, z-1$  #9  $x+1, y+1, z$

**Table 4.** Complete list of bond lengths [ $\text{\AA}$ ] and angles [deg] for  $[\text{C}_{28}\text{H}_{24}\text{N}_4](\text{NO}_3)_2 \cdot 2\text{H}_2\text{O}$  ( $2 \cdot 2\text{H}_2\text{O}$ )

N(2)-C(10)	1.329(4)	N(1)-C(1)	1.315(5)
N(2)-C(9)	1.351(4)	N(3)-O(3)	1.152(5)
N(2)-C(11)	1.497(3)	N(3)-O(1)	1.181(5)
C(6)-C(8)	1.390(4)	C(14)-C(13)#1	1.397(4)
C(5)-C(4)	1.138(5)	C(12)-C(14)	1.384(4)
C(10)-N(2)-C(9)	119.9(2)	O(3)-N(3)-O(2)	120.6(5)
N(2)-C(10)-C(8)	121.4(3)	N(1)-C(1)-C(3)	124.9(4)
N(2)-C(9)-C(7)	121.1(3)	C(12)-C(13)-C(14)#1	121.4(3)
C(1)-N(1)-C(2)	115.1(3)	N(1)-C(1)-C(3)	124.9(4)
N(1)-C(2)-C(4)	125.1(4)	C(12)-C(14)-C(13)#1	119.6(3)

Symmetry antiformations used to generate equivalent atoms: #1  $-x+1, -y+1, -z+1$

**Table 5.** Hydrogen bonds for compound  $2 \cdot 2\text{H}_2\text{O}$  [ Å and °].

D-H...A	d(D...H)	d(H...A)	d(D...A)	<(DHA)
O(4)-H(30)...O(1)	0.98	2.41	3.199	136
O(4)-H(30)...O(2)	0.98	1.97	2.924	162
C(1)-H(1)...O(3)#1	1.08	2.44	3.202	127
C(7)-H(7)...O(3)	1.08	2.44	3.412	149
C(9)-H(9)...N(1)#2	1.08	2.41	3.443	158
C(10)-H(10)...O(2)#3	1.08	2.37	3.218	135
C(11)-H(11B)...O(2)#3	1.08	2.37	3.338	147

Symmetry antiformations used to generate equivalent atoms:

#1  $-1+x, y, z$  #2  $3/2+x, 1/2-y, 1/2+z$  #3  $3/2-x, 1/2+y, 1/2-z$

**Table 6.** NBO analysis of some selected bonds of compound **2**; *anti*, *intermediates*.(1N-24C-52C-29N= -120°, -90°, -60°) and *syn* conformers of compound **1**

Donor NBO (i)	Acceptor NBO (j) Compound <b>2</b>	Stabilization Energy $E^2$ (i,j) (kcal/mol)	H-bond distance (Å)
63 O [LP]	55C-56H [BD*]	6.55	2.142
64 O [LP]	37C-38H [BD*]	14.41	1.943
64 O [LP]	34C-35H [BD*]	7.46	2.136
58 O [LP]	9C-10H [BD*]	21.46	1.833
58 O [LP]	27C-28H [BD*]	2.99	2.184
59 O [LP]	6C-7H [BD*]	5.74	1.992
59 O [LP]	9C-10H [BD*]	1.00	2.376
<b>Anti conformer of compound 1</b>			
62 F [LP]	27C-28H [BD*]	1.61	2.225
63 F [LP]	27C-28H [BD*]	0.06	2.582
64 F [LP]	9C-10H [BD*]	6.07	2.183
67 F [LP]	37C-38H [BD*]	2.94	2.183
67 F [LP]	39C-40H [BD*]	0.12	2.804
68 F [LP]	55C-56H [BD*]	3.30	2.224
69 F [LP]	37C-38H [BD*]	6.07	2.057
69 F [LP]	34C-35H [BD*]	4.88	2.143
69 F [LP]	55C-56H [BD*]	0.51	2.583

70 F [LP]	55C-56H [BD*]	1.60	2.443
<b>Intermediate conformer of compound 1</b>			
<b>1N-24C-52C-29N=-120°</b>			
61 F [LP]	32C-33H [BD*]	4.31	2.181
61 F [LP]	34C-36H [BD*]	1.99	2.255
62 F [LP]	32C-33H [BD*]	3.37	2.148
63 F [LP]	4C-5H [BD*]	2.99	2.222
66 F [LP]	6C-8H [BD*]	1.94	2.148
66 F [LP]	9C-10H [BD*]	5.03	2.103
68 F [LP]	25C-26H [BD*]	2.37	2.250
69 F [LP]	9C-10H [BD*]	3.62	2.164
<b>Intermediate conformer of compound 1</b>			
<b>1N-24C-52C-29N=-90°</b>			
60 F [LP]	4c-42H [BD*]	3.80	2.217
61 F [LP]	32C-33H [BD*]	1.99	2.261
63 F [LP]	4C-5H [BD*]	8.13	2.060
66 F [LP]	6C-8H [BD*]	3.83	2.190
66 F [LP]	9C-10H [BD*]	5.38	2.080
66 F [LP]	25C-26H [BD*]	0.97	2.486
68 F [LP]	25C-26H [BD*]	4.70	2.167

69 F [LP]	9C-10H [BD*]	3.33	2.170
<b>Intermediate conformer of compound 1</b> <b>1N-24C-52C-29N=-60°</b>			
58 F [LP]	13C-14H [BD*]	1.66	2.396
60 F [LP]	4c-42H [BD*]	4.50	2.162
60 F [LP]	45C-46H [BD*]	2.29	2.405
61 F [LP]	32C-33H [BD*]	2.46	2.238
63 F [LP]	4C-5H [BD*]	8.06	2.059
66 F [LP]	9C-10H [BD*]	5.50	2.078
66 F [LP]	6C-8H [BD*]	2.98	2.200
68 F [LP]	25C-26H [BD*]	4.56	2.174
69 F [LP]	9C-10H [BD*]	3.37	2.174
<b>Syn conformer of compound 1</b>			

58 F [LP]	17C-18H [BD*]	3.75	2.273
58 F [LP]	13C-14H [BD*]	1.17	2.367
60 F [LP]	39C-40H [BD*]	2.84	2.280
62 F [LP]	37C-38H [BD*]	4.96	2.176
62 F [LP]	53C-54H [BD*]	1.73	2.319
63 F [LP]	4C-5H [BD*]	0.55	2.532
63 F [LP]	27C-28H [BD*]	1.23	2.461
66 F [LP]	9C-10H [BD*]	4.92	2.179
66 F [LP]	25C-26H [BD*]	1.73	2.319
67 F [LP]	32C-33H [BD*]	0.53	2.545
67 F [LP]	55C-56H [BD*]	1.25	2.454
69 F [LP]	1c-12H [BD*]	2.87	2.278
70 F [LP]	4c-42H [BD*]	1.17	2.366
70 F [LP]	45C-46H [BD*]	3.67	2.277

**Table 7.** Calculated values of equilibrium constants (K) at different temperature (in Kelvin) of different equilibrium exist between the different conformers of cationic receptor **c** and compound **1**.

Temp (K)	Antic $\rightleftharpoons$ syn <b>c</b>	Syn1 $\rightleftharpoons$ Anti1	Intermediate (-60°) $\rightleftharpoons$ Anti 1	Intermediate (-90°) $\rightleftharpoons$ Anti 1	Intermediate (-120°) $\rightleftharpoons$ Anti1
100	0.00004	0.00000	0.00000	0.00000	-
150	0.00071	0.00000	0.00000	0.00031	928
200	0.00286	0.00000	0.00000	0.00362	269
250	0.00663	0.00000	0.00003	0.01586	128
300	0.01160	0.00000	0.00027	0.04232	78
350	0.01730	0.00000	0.00134	0.08510	55
400	0.02334	0.00001	0.00441	0.14345	42
450	0.02946	0.00010	0.01113	0.21506	34
500	0.03548	0.00054	0.02331	0.29707	29
550	0.04131	0.00214	0.04266	0.38670	26
600	0.04689	0.00676	0.07057	0.48149	23
650	0.05219	0.01791	0.10798	0.57941	21
700	0.05720	0.04127	0.15545	0.67885	19
750	0.06193	0.08505	0.21313	0.77853	18
800	0.06638	0.16010	0.28085	0.87752	17

## For Table of Contents Use Only

# An Organic Receptor Isolated in an Unusual Intermediate Conformation: Computation, Crystallography and Hirshfeld Surface Analysis

Indravath Krishna Naik, Rudraditya Sarkar, Vedichi Madhu, Ramababu Bolligarla, Ravada Kishore and Samar K. Das\*

Artwork

